Cross-Layer Analysis and Optimization on Access Delay in Channel-Hopping-Based Distributed Cognitive Radio Networks

Jiaxun Li, Haitao Zhao, *Senior Member, IEEE*, Shaojie Zhang, Abdelhakim Senhaji Hafid, *Member, IEEE*, Dusit Niyato, *Fellow, IEEE*, and Jibo Wei, *Member, IEEE*

***Abstract*— In channel-hopping (CH)-based distributed cognitive radio networks (CRNs), the time duration that secondary users (SUs) spend for establishing communication links is called access delay. To evaluate access delay, we propose an access delay model by jointly considering imperfect spectrum sensing and multi-channel multi-SU transmission, from the cross-layer perspective. The model considers two typical scenarios. The first scenario assumes that the SUs do not use contention scheme (CS) which indicates that the time slot is relatively shorter to just allow a transmission. The second scenario assumes that the SUs employ CS [i.e., modified Distributed Coordination Function (DCF)-based Carrier Sense Multiple Access/Collision Avoidance (CSMA/CA) in this paper], which indicates that the time slot is long enough to regulate multiple transmissions. We then propose a bio-inspired algorithm for the first scenario and a self-adaptive step-length algorithm for the second scenario to search for the optimal values of spectrum sensing parameters. The theoretical analysis and simulation results validate the proposed access delay model and show that the proposed algorithms can reduce the most redundant computation. They also show that the optimization of cross-layer parameters can significantly decrease SUs' access delay. Moreover, we conduct a cost-benefit analysis to evaluate the performance of the two scenarios.**

***Index Terms*— Blind rendezvous, cognitive radio networks, channel-hopping, optimization, spectrum sensing.**

I. Introduction

COGNITIVE radio (CR) has emerged as an advanced and promising technology to exploit wireless spectrum opportunistically. In CRNs, any pair of SUs are required to locate each other on the spectrum to establish a communication link, which is referred to as 'rendezvous' [1]. Typically, employing a dedicated common control channel (CCC) is manageable and effective to exchange rendezvous information. Hence, most early works use CCC [2]–[4] to facilitate the rendezvous process. However, the CCC design may be inflexible or even fragile in highly dynamic networks scenarios, especially in distributed CRNs. Thus, various CH algorithms, which do not rely on any preassigned controller or CCC, have been widely studied to tackle the rendezvous problem in distributed CRNs. In these works [1], [5]–[10], [19]–[21], [26], a sender SU and a receiver SU are described as *Achieve Rendezvous* if they hop on a same channel in the same time slot. The amount of time that they spend for achieving rendezvous is called *Time To Rendezvous* (TTR). Even though CH-based rendezvous schemes can overcome the drawbacks introduced by CCC-based rendezvous schemes, TTR of CH scheme is relatively longer due to the fact that SUs with CH scheme have to hop on and access every available channel for any potential rendezvous [9]. Hence, the key objective in designing CH scheme is to minimize TTR. Most of these designs focus on developing an effective CH sequence [1], [5]–[10], [19], [20], [26]. However, SUs that achieve rendezvous cannot always communicate with each other because of transmission collision caused by multiple SUs hopping on a same channel and transmitting at the same time. In this paper, the time duration taken by a pair of SUs for establishing a communication link (i.e., successfully exchanging rendezvous information) is called access delay. In distributed CRNs, the first step for SUs is to establish communication links with each other. In this sense, access delay is an important metric to evaluate performance of forming distributed CRNs.

Contention scheme (CS) such as Distributed Coordination Function (DCF) based Carrier Sense multiple Access/Collision Avoidance (CSMA/CA), which allows multiple SUs to transmit within the same time slot in a distributed manner, is employed in many works to avoid collision [5]–[10], [17]–[21], [27]. However, in this case, a long enough duration has to be reserved in the time slot for SUs to contend for transmission opportunities. Then, the access delay in CH with CS (CHCS) may be large because it may take SUs

Manuscript received July 22, 2018; revised November 30, 2018 and February 4, 2019; accepted February 18, 2019. This work is supported in part by National Natural Science Foundation of China under grant No. 61471376. The associate editor coordinating the review of this paper and approving it for publication was D. Marabissi. *(Corresponding author: Haitao Zhao.)*

J. Li, H. Zhao, and J. Wei are with the College of Electronic Science and Engineering, National University of Defense Technology, Changsha 410073, China (e-mail: lijiaxun@nudt.edu.cn; haitaozhao@nudt.edu.cn).

S. Zhang is with the Army Aviation Institute of PLA, Beijing 101149, China (e-mail: zhangshaojie@nudt.edu.cn).

A. S. Hafid is with the Department of Computer Science and Operations Research, University of Montreal, Quebec, H3C 3J7, Canada (e-mail: ahafid@iro.umontreal.ca).

D. Niyato is with the School of Computer Science and Engineering, Nanyang Technological University, Singapore 639798, and also with the School of Physical and Mathematical Sciences, Nanyang Technological University, Singapore 639798 (e-mail: dniyato@ntu.edu.sg).

Color versions of one or more of the figures in this paper are available online at http://ieeexplore.ieee.org.

Digital Object Identifier 10.1109/TCOMM.2019.2903112

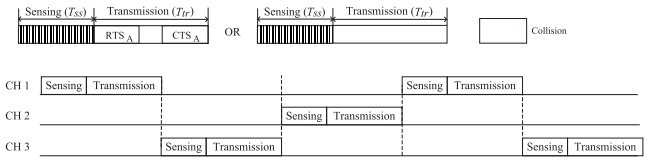

(a) Transmission pattern for CHNCS

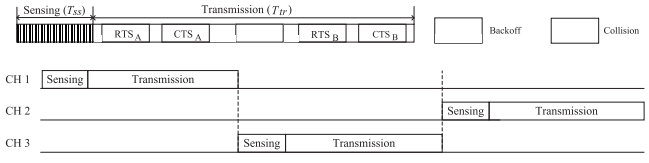

(b) Transmission pattern for CHCS

Fig. 1. Transmission patterns for CHCS and CHNCS scenarios.

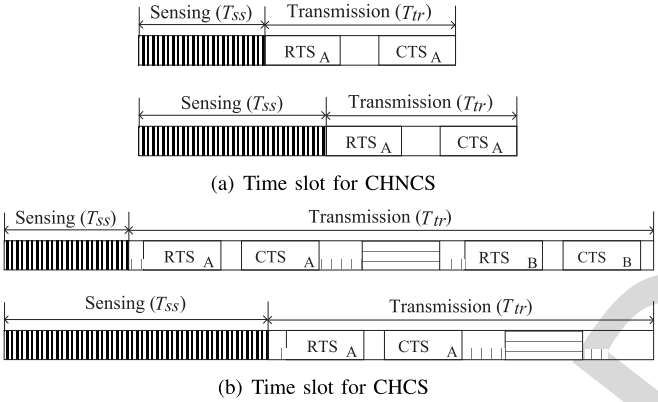

(a) Time slot for CHNCS

(b) Time slot for CHCS

Fig. 2. Structures of time slot with different sensing durations for CHCS and CHNCS.

multiple slots to achieve rendezvous with target SUs. In CH without CS (CHNCS), the time slot can be relatively short for only allowing one transmission of rendezvous information; thus, SUs may establish communication links with smaller access delay. The differences between these two scenarios are depicted in Fig. 1. As depicted in Fig. 1 (a), in CHNCS scenario, the transmission duration of a time slot only contains a RTS/CTS transmission or collision by multi-SU transmission. However, for CHCS in Fig. 2 (b), though there may also exist collisions during transmission duration in the time slot, SUs may still successfully transmit RTS/CTS within the transmission duration; this is because that large transmission duration is reserved to allow multiple transmissions by using CSMA/CA. Comparing Fig. 1 (a) and (b), CHNCS has short duration of time slot but is easy to cause collision while CHCS allows multiple transmissions but has long transmission duration. Hence, impacts of length of time slot and CS in CH on access delay should be analyzed to evaluate the performance of access delay in both CHCS and CHNCS scenarios.

In order to protect primary users' (PU) transmissions, SUs have to perform spectrum sensing to sense PUs' activities on channels and avoid interferences. However, it is likely for SUs to perform imperfect spectrum sensing in practice. Once imperfect spectrum sensing occurs, SUs will either not access an idle channel (false detection) or access a channel that PUs are using (miss detection).

The structures of time slot with different sensing durations for CHCS and CHNCS are shown in Fig. 2. On the one hand,long enough duration of spectrum sensing can provide accurate sensing results that contribute to protect PUs and avoid wasting transmission opportunities in both CHCS and CHNCS. On the other hand, in the case of CHNCS, as shown in Fig. 2 (a), long spectrum sensing time results in long time slot, which may increase access delay; in the case of CHCS, as shown in Fig. 2 (b), long spectrum sensing time results in short contention time whereas multiple SUs should be given long enough time to use CS for exchanging rendezvous information on the rendezvous channel.

In this paper,[1] we formulate the access delay model and propose corresponding optimization algorithms for both CHCS and CHNCS scenarios. The main contributions are as follows.

- We formulate the novel access delay model based on the assumptions that SUs employ CS (i.e., CHCS) and that SUs do not employ CS (i.e., CHNCS) respectively, in CH based rendezvous; the model jointly considers the impacts of imperfect spectrum sensing, specific CH algorithm and multi-SU transmission under the constraint of interference to PUs.
- We propose a methodology to analyze the number of time slots consumed for rendezvous of CH algorithms, and derive closed-form expressions of average number of time slots consumed for the first rendezvous and successive rendezvous.
- We propose a bio-inspired algorithm which employs the firefly algorithm [13] to quickly search the optimal parameters (i.e., sensing duration and detection threshold) for CHNCS; we propose an algorithm which can autonomously adjust step-length for searching optimal parameters (i.e., sensing duration) for CHCS.
- We investigate the benefit and cost of establishing communication links using CHNCS over CHCS in terms of access delay and analyze performance of both CHNCS and CHCS under different scenarios where there exist different number of SUs and channels.

The rest of the paper is organized as follows. Section II reviews related work. Section III describes the system model and outlines the access delay problem. Section IV presents analysis of multi-channel multi-SU access for both CHNCS and CHCS. Section V presents analysis of channel hopping algorithm where Sender Jump-Receiver Wait (SJ-RW) [9] is taken as an example. Section VI presents optimization algorithms on access delay for both CHNCS and CHCS. Section VII presents simulation results and discusses impacts of number of SUs and channels. Finally, Section VIII concludes the paper.

II. Related Work

There exist some works focusing on delay analysis and optimization in CRNs [14]–[16], [23], [27]. Wang *et al.* [14] study SUs' queueing delay performance by taking a fluid queue approximation approach in which queue dynamics is

[1]The part of the work studied in this paper is submitted to IEEE Globecom 2018 and is accepted.

TABLE I
MAIN NOTATIONS AND DEFINITIONS

Notation	Definition	Notation	Definition
P_{tra}	Probability of SU(s) transmitting in a time slot	T_{slot}	Total duration of SUs' time slot
τ	SUs' conditional transmission probability	$\overline{T_{AD}}$	Access delay
T_{ss}	Time duration of spectrum sensing	M	Number of channels in CRNs
T_{tr}	Time duration of transmission period	N	Number of SUs in CRNs
T_{rt}	Time duration of Reserve Time in CHCS	ε	The detection threshold
T_{tx}	Time duration of a transmission in CHCS	W	Minimum contention window
P_b	Probability that channel is busy for SUs	m	Maximum backoff stage
P_i	Probability that channel is idle for SUs	p	Probability of a failed transmission
f_s	The sampling frequency of SUs in spectrum sensing	P_d	Probability of detection
γ	PUs' signal-to-noise ratio (SNR) received by SUs	P_f	Probability of false detection
P_I	Probability of interference probability to PUs	P_m	Probability of miss detection
P_{ERI}	Probability of SUs exchanging rendezvous information	P_{CSI}	Probability of sensing channel as idle
$P(n_s)$	Probability of n_s SUs achieving rendezvous on a channel	P_{BL}	Probability of establishing a link

represented as Poisson driven stochastic differential equations. Liang *et. al* [15] derive the average packet transmission delay for periodic switching channel scheme and triggered switching channel scheme, besides, for each switching scheme, they consider two types of real-time traffic, i.e., random burst of packets and Poisson arrival of packets. Even though these two works both consider multi-user contention in analyzing delay, they all assume that the spectrum sensing is perfect. Li *et al.* [16] analyze the expected per-hop delay incorporating the sensing delay and transmission delay in multi-hop multi-flow CRNs, considering imperfect spectrum sensing and transmission contention, but the analysis lacks of consideration of spectrum access mechanism (e.g., CCC or CH). Moreover, there is a type of delay resulted from the specific characteristics of designing an opportunistic spectrum access scheme in CRNs, e.g., [23], [27]. Hossain and Sarkar [23] propose a MAC scheme for CH based rendezvous with analysis of medium access delay and queueing delay; though it is claimed that quorum CH algorithm is used to establish the rendezvous, the impact of neither CH algorithm nor imperfect spectrum sensing on delay is considered. Liu *et al.* [27] analyze the impacts of rendezvous failure and neighbor contention on optimizing time slot and propose a simple MAC scheme for slot-asynchronous CH based rendezvous. However, the analysis is mainly based on the assumption of one neighbor SU, and the analysis also lacks of consideration of imperfect spectrum sensing and specific CH algorithm.

On the other hand, the increasing number of applications motivates the research on rendezvous-guaranteed CH sequence design (e.g., [1], [5]–[10], [19], [20], [26]). These works can be mainly divided into two categories: A) the design is based on the system or theory with inherent attribute like rotation closure property (RCP) which can achieve guaranteed rendezvous with different delay offsets [e.g., disjoint difference set [5], quorum system [7], [19], balanced incomplete block design (BIBD) [10], [20]], and B) the design is based on partially-random scheme with set pattern like jump-stay (hop-wait) mainly employing Mod operation, e.g., [1], [6], [8] and [9]. However, all above works fail to consider the impact of multi-SU transmission (e.g., collision). Therefore, Liu and Xie [21] analyze impact of collision and congestion on performance of rendezvous. They further develop a framework which can optimize system parameters to adapt to the dynamic network. However, they do not take into consideration the impacts, in practice, of detailed CH sequence and rendezvous scenarios.

Though the related works mentioned above focus on different aspects of CRNs, they fail to jointly take into consideration the impact of detailed operations in PHY layer (i.e., imperfect spectrum sensing) and MAC layer (i.e., exchanging information/data with specific CH or CCC scheme). Considering detailed operations surely helps performance evaluation more accurate.

III. SYSTEM MODEL AND PRELIMINARIES

For better readability, Table I shows the key notations used in describing our proposal. In this paper, we use different superscripts (i.e., ncs for CHNCS and cs for CHCS) to identify different functions and expressions which represent the same meaning.

We consider a distributed CRN where there are N SUs coexisting with PUs in the same geographical area. All SUs and PUs share the same set of non-overlapping M channels, and they all communicate with each other using a time-slotted method. Each SU is equipped with a half-duplex radio which is capable of detecting channel availability and switching among these M channels. Given that the channel switch overhead is in the order of microseconds [24] and the duration of a time slot is in the order of milliseconds (e.g., 10 ms in IEEE 802.22 [11]), we consider that the channel switch overhead is negligible.

SUs in distributed CRN are assumed to rendezvous with each other and further establish communication links. As shown in Fig. 3, a sender SU first senses the channel that it hops on. If the channel is sensed as idle, then the sender SU sends the rendezvous request (e.g., RTS) to try to establish a communication link with its receiver SU. If the sender SU receives the rendezvous acknowledgement (e.g., CTS) from its receiver SU successfully, this pair of SUs setup the link. However, if the channel is sensed as busy or the sender SU fails to receive the rendezvous acknowledgement in current time slot, it then hops on another channel in the next time slot and continues the sensing-access process. Hence, each time slot for both CHNCS and CHCS is composed of two parts:

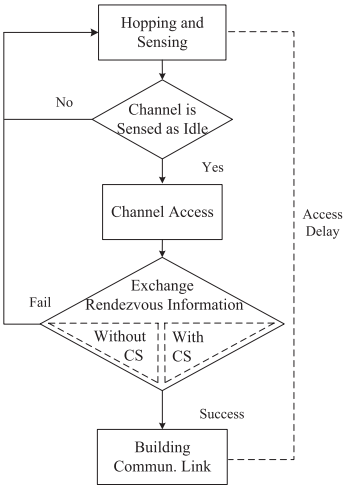

Fig. 3. Sensing-access process to establish communication link with CH scheme in multi-SU CRN.

spectrum sensing duration T_{ss} and transmission duration T_{tr} (shown in Figs. 1 and 2), i.e.,

$$T_{slot} = T_{ss} + T_{tr}. \tag{1}$$

In CRNs, channel state is determined by PUs' activities. The PU's traffic is modeled as a 1-0 renewal process [12] where "1" represents that the channel is busy in a time slot and "0" represents the channel is idle. To simplify the analysis, we assume that the channel state is steady during the time slot and the average time holding for state "1" is α and β for state "0". Therefore, in any time slot, the channel is busy with probability $P_b = \frac{\alpha}{\alpha+\beta}$ and idle with probability $P_i = \frac{\beta}{\alpha+\beta}$.

It is worth noting that the objective is to minimize access delay by optimizing both PHY and MAC parameters in CH-based multi-channel multi-SU distributed CRNs. Indeed, we do not consider data throughput (i.e., data transmission in a time slot) in the proposed access delay model. Hence, we assume that SUs, during T_{tr}, attempt to exchange only rendezvous information. Data transmission operations can be performed by SUs with some specific protocols ([3], [11]). This assumption minimizes the impact of data transmission scheme on establishing communication links. Thus, we can establish a general purpose access delay model, which can be easily adapted to different protocols with specific transmission schemes.

A. Spectrum Sensing

To make the proposed optimization approach generally applicable, we adopt the widely used energy detection scheme [11], [12], [22] to perform spectrum sensing. Therefore, according to [12], the probability of false detection is then given by

$$P_f(\varepsilon, T_{ss}) = \Pr(Y > \varepsilon | H_0) = \frac{1}{2}\mathrm{erfc}\left(\frac{\varepsilon - f_s T_{ss}}{2\sqrt{f_s T_{ss}}}\right), \tag{2}$$

where Y is the sensing result which is the sum of samples, ϵ denote the detection threshold, f_s represent the sampling frequency, H_0 denotes the hypothesis that the licensed channel is unoccupied and $\mathrm{erfc}(\cdot)$ is the complementary error function of the standard Gaussian [22]. Under hypothesis H_1 that the PU is active on the licensed channel, let $\gamma = \sigma_s/\sigma_n$ denote the PUs' signal-to-noise ratio (SNR) measured at the SUs' receiver; the probability of detection can be derived as

$$P_d(\varepsilon, T_{ss}) = \Pr(Y > \varepsilon | H_1) = \frac{1}{2}\mathrm{erfc}\left(\frac{\varepsilon - f_s T_{ss}(1+\gamma)}{2\sqrt{f_s T_{ss}(1+2\gamma)}}\right), \tag{3}$$

and the probability of miss detection can be expressed as

$$P_m(\varepsilon, T_{ss}) = \Pr(Y < \varepsilon | H_1) = 1 - P_d(\varepsilon, T_{ss}). \tag{4}$$

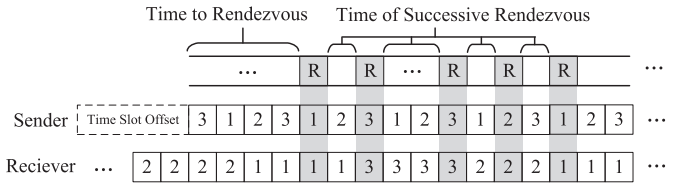

Fig. 4. Illustration of TTR and TSR. The "R" in gray blocks means the rendezvous time slots and numbers represent channel indices.

B. Access Delay

If the sender SU wants to establish a communication link with its receiver SU, they should first achieve rendezvous by following CH sequences. The process is depicted in Fig. 4, where SUs spend *Time To Rendezvous* (*TTR*) to achieve first rendezvous, or they have to spend *Time of Successive Rendezvous* (*TSR*) for each rendezvous after they fail to achieve the first rendezvous. The success or failure of each rendezvous relates to two conditions: 1) Access the channel as SUs sense the channel is idle (with probability P_{CSI}), and 2) SUs exchange RTS/CTS successfully on the rendezvous channel (with probability P_{ERI}).

P_{CSI} relates to PUs' activity and SUs' sensing results. If Y is smaller than ϵ, the channel is idle; this can be represented as $P_{CSI} = \mathrm{P_r}(Y < \varepsilon)$. Considering miss detection, false detection and PUs' activities, the probability of channel being sensed idle is expressed as

$$\begin{aligned} P_{CSI} &= \Pr(Y < \varepsilon | H_0)\Pr(H_0) + \Pr(Y < \varepsilon | H_1)\Pr(H_1) \\ &= (1 - P_f(\varepsilon, T_{ss})) \cdot P_i + P_m \cdot P_b. \end{aligned} \tag{5}$$

Let "A" denote the event that the channel sensed by a SU is idle and "E" denote the event that the SU succeeds in transmission contention. The probability P_{BL} that the SU establishes a communication link with its receiver can be expressed as

$$\begin{aligned} P_{BL} &= \Pr(\mathrm{AE}) = \Pr(\mathrm{A})\Pr(\mathrm{E}|\mathrm{A}) \\ &= P_{CSI}(\varepsilon, T_{ss}, T_{tr}) \cdot P_{ERI}(\varepsilon, T_{ss}, T_{tr}), \end{aligned} \tag{6}$$

where $P_{ERI}(\varepsilon, T_{ss}, T_{tr})$ represents $\Pr(\mathrm{E}|\mathrm{A})$.

Furthermore, let *ATTR* represent the average number of time slots that SUs take for achieving the first rendezvous, and let *ATSR* denote average number of time slots taken for successive

rendezvous, then expected access delay $\overline{T_{AD}}$ for CHNCS can be expressed as

$$\begin{aligned}\overline{T_{AD}^{ncs}} &= T_{slot}\cdot[(ATTR+1)P_{BL} \\ &\quad + \sum_{n=1}^{\infty} P_{BL}(1-P_{BL})^n(ATTR+1+n(ATSR+1))] \\ &= T_{slot}^{ncs}\cdot[ATTR+1+\frac{1-P_{BL}^{ncs}}{P_{BL}^{ncs}}\cdot(ATSR+1)].\end{aligned} \tag{7}$$

where T_{slot} represents the duration of the time slot. Similarly, for CHCS, the access delay is

$$\overline{T_{AD}^{cs}} = T_{slot}^{cs}\cdot[ATTR+1+\frac{1-P_{BL}^{cs}}{P_{BL}^{cs}}\cdot(ATSR+1)]+\overline{\Delta}, \tag{8}$$

where $\overline{\Delta}$ is average time duration consumed for contention in the rendezvous time slot.

Both Eq. 13 and Eq. 14 indicate that SUs on average undergoes $\frac{1-P_{BL}^{cs}}{P_{BL}^{cs}}$ rendezvous failures including failure in first attempt of rendezvous. The difference of access delay between CHCS and CHNCS lies on whether CS is employed or not, i.e., T_{slot}, $P_{ERI}(\varepsilon, T_{ss}, T_{tr})$ and $\overline{\Delta}$.

IV. Analysis of Transmission in a Time Slot

In distributed CRNs, SUs are likely to randomly select CH sequences generated by CH algorithm. Some existing CH algorithms [5], [7], [9], [10], [19], [20] are able to regulate SUs to hop uniformly between channels. Hence, we assume that each SU hops on and senses a specific channel with probability $1/M$. Then, the probability that the other n_s SUs hop on and sense the same channel with the corresponding SU can be expressed as

$$P(n_s)=C_{N-1}^{n_s}\cdot\left(\frac{1}{M}\right)^{n_s}\cdot\left(\frac{M-1}{M}\right)^{N-1-n_s}, \quad n_s\le N-1. \tag{9}$$

Once multiple SUs hop on the same channel and sense it as idle, they will transmit RTS/CTS immediately in the case of CHNCS or contend for the channel in the case of CHCS. In both scenarios, the SUs suffer from two kinds of failed transmissions: (a) collisions with SU's and/or PUs' transmissions and (b) SUs fail to achieve rendezvous.

Let P_c denote the probability of transmission collision, P_c can be expresses as

$$P_c = P_c^s + P_c^p - P_c^s\cdot P_c^p, \tag{10}$$

where P_c^s (P_c^p) is the probability that the transmission collides with other SUs' (PUs') transmissions. Collisions with other SUs occur only when at least one of the n_s SUs transmit. Let τ denote the transmission probability; P_c^s can be expressed as

$$P_c^s = \sum_{n_s=1}^{N-1} P(n_s)\cdot(1-(1-\tau)^{n_s}). \tag{11}$$

The transmission collides with PUs' transmissions only when miss detection occurs. Then, P_c^p can be expresses as

$$P_c^p = P_m(\varepsilon, T_{ss})\cdot P_b. \tag{12}$$

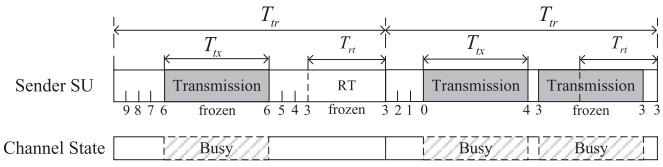

Fig. 5. Transmission scheme of IEEE 802.11 DCF adopted in CH-based CRNs.

A. Multi-SU Transmission for CHNCS

In the CHNCS scenario, SUs only need to transmit RTS/CTS for one time during the entire duration of the time slot. Hence, T_{tr} is fixed and can be expressed as

$$T_{tr}^{ncs} = t_{RTS} + t_{CTS} + \text{SIFS}, \tag{13}$$

where t_{RTS} and t_{CTS} denote the transmission duration of RTS and CTS respectively; SIFS is short for 'short interframe space' defined in IEEE 802.11 standard.

Due to the fact that SUs in CHNCS will transmit immediately once they sense the channel idle, τ for CHNCS in Eq. (11) can be expressed as

$$\tau^{ncs} = 1. \tag{14}$$

Then, $P_{ERI}(\varepsilon, T_{ss}, T_{tr})$ for CHNCS can be expressed as

$$P_{ERI}^{ncs}(\varepsilon, T_{ss}, T_{tr}) = 1 - P_c(\tau^{ncs}). \tag{15}$$

B. Multi-SU Transmission for CHCS

In the CHCS scenario, SUs employ CS to transmit RTS/CTS on the same channel distributedly. Since IEEE 802.11 DCF-based CSMA/CA has been widely used in distributed wireless networks, we adopt the CS which is similar to IEEE 802.11 DCF to regulate the transmissions in CHCS. As the same in IEEE 802.11 DCF, when the backoff counter decreases to zero, the SU starts to transmit; otherwise, it continues to decrease its backoff counter or freezes the counter when it detects other SUs transmitting.[2] The difference is that, in conventional wireless networks, users do not need to hop between channels during the contention-transmission process, while, with slot-by-slot structure in multi-channel CRNs, SUs have to hop on different channels after a fixed period (i.e., T_{slot}). It may happen that after an SU wins a transmission opportunity by CS, the time left in this time slot is not enough for the transmission. To avoid this, a Reserve Time (RT) (denoted by T_{rt}) which has a minimal duration required for exchanging RTS/CTS is placed in the end of each time slot (see Fig. 5, for better clarity, the sensing operation is ignored). Then, the durations of a transmission and RT are expressed as

$$T_{tx} = t_{RTS} + t_{CTS} + \text{SIFS} + \text{DIFS} \tag{16a}$$

$$T_{rt} = t_{RTS} + t_{CTS} + \text{SIFS}. \tag{16b}$$

[2]To avoid the channel busy time-inconsistency problem [17], each SU freezes its backoff counter for a duration of T_{tx} when it detects a transmission that is no matter successful or not.

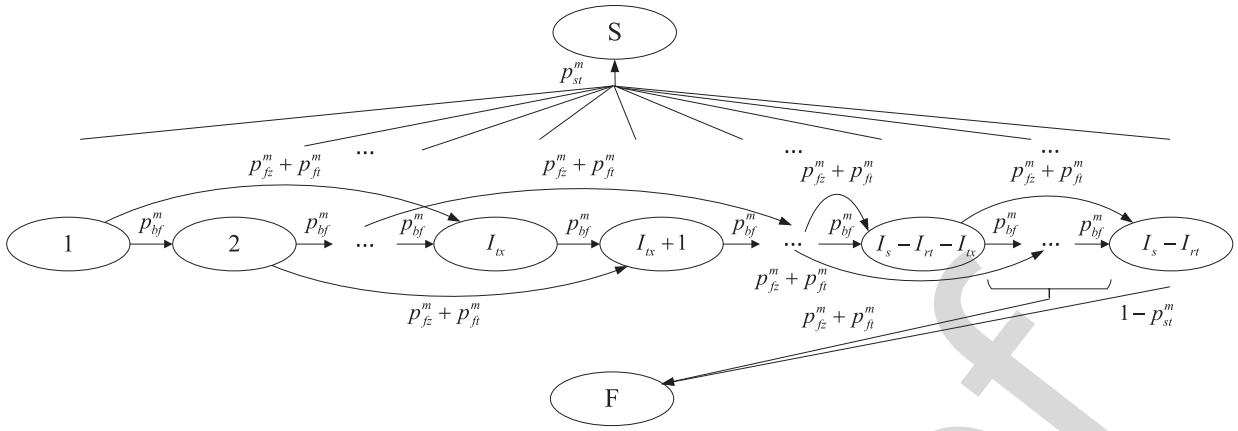

Fig. 6. State transition process of the corresponding SU in one time slot.

To derive $P_{ERI}^{cs}(\varepsilon, T_{ss}, T_{tr})$, we model the contention-transmission process as an absorbing Markov chain. The duration of T_{tr}^{cs} is subdivided into I_s backoff slots to construct a discrete time system; all backoff slots in each T_{tr}^{cs} are labeled as $1, \ldots, I_s$. Correspondingly, the durations of T_{rt}^{cs} and T_{tx}^{cs} are subdivided into I_{rt} and I_{tx} bakcoff slots, respectively. Note that if SUs fail to seize the opportunity within the first $(I_s - I_{rt})$ backoff slots, they will fail to establish communication links in current time slot. Hence, we only consider these $(I_s - I_{rt})$ backoff slots.

During transmission contention process, as shown in Fig. 6, SUs may encounter one of the four possible events: 1) backoff operation, with probability p_{bf}; 2) backoff counter frozen due to other SUs' transmissions, with probability p_{fz}; 3) a failed transmission of the corresponding SU, with probability p_{ft}; and 4) a successful transmission of the SU, with probability p_{st}. The probabilities of the four events can be expressed as

$$p_{bf} = (1-\tau) \cdot \sum_{n_s=0}^{N-1} P(n_s) \cdot (1-\tau)^{n_s} \tag{17a}$$

$$p_{st} = \tau \cdot \sum_{n_s=0}^{N-1} P(n_s) \cdot (1-\tau)^{n_s} \tag{17b}$$

$$p_{fz} = (1-\tau) \cdot \sum_{n_s=1}^{N-1} P(n_s) \cdot (1-(1-\tau)^{n_s}) \tag{17c}$$

$$p_{ft} = \tau \cdot \sum_{n_s=1}^{N-1} P(n_s) \cdot (1-(1-\tau)^{n_s}). \tag{17d}$$

According to Bianchi's research [29], τ in Eqs. (11) and (17) can be derived as

$$\tau^{cs} = \frac{2\,(1-2p^{cs})}{(1-2p^{cs})\,(W+1) + p^{cs} W\,(1-(2p^{cs})^m)}, \tag{18}$$

where W denotes the minimum contention window, m denotes the maximum backoff stage and p^{cs} is the probability of a failed transmission. Considering failed transmissions due to failed rendezvous, p^{cs} can be expressed as

$$p^{cs} = 1 - (1-P_c) \cdot P_{ren}, \tag{19}$$

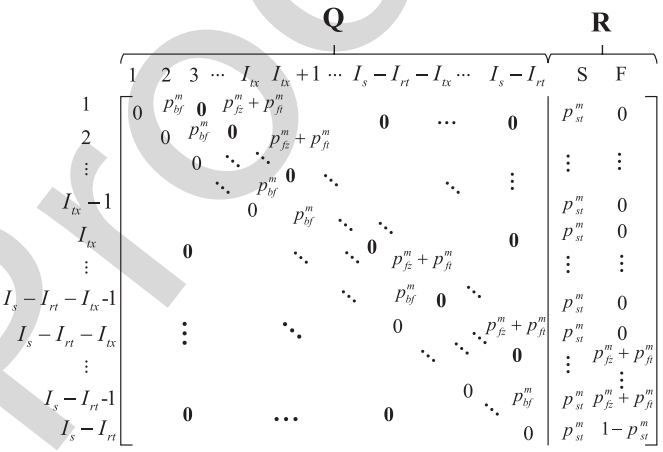

Fig. 7. One-step transition probability matrix of the absorbing Markov chain.

where P_{ren} represents the probability that SUs achieve rendezvous (details are in Section V).

In Fig. 6, SUs finally falls into one of the two absorbing states: 1) "S": successfully establishing a communication link in current time slot and 2) "F": failing to establish a communication link. We can formulate the canonical form of one-step transition probability matrix P as

$$\mathrm{P} = \begin{bmatrix} \mathrm{Q} & \mathrm{R} \\ 0 & \mathrm{I} \end{bmatrix}, \tag{20}$$

where I is the identity matrix and R is the probability matrix of sates "S" and "F" (see Fig. 7).

According to the Markov chain theory [30], the n-step transition probability matrix without absorbing states can be expressed as Q^n in which the element $(\mathrm{Q}^n)_{i,j}$ is the (ij)th entry of the matrix. $(\mathrm{Q}^n)_{ij}$ is also the probability that a SU transits from $state\ i$ to $state\ j$ with n steps. Thus, the probability p_{ij}^I that an SU transits from $state\ I_i$ to $state\ I_j$ can be expressed as

$$p_{ij}^I = \sum_{k=0}^{\infty} \left(\mathrm{Q}^k\right)_{ij}. \tag{21}$$

Let P^I denote the transition probability matrix which is composed of elements p_{ij}^I $(1 \le i,j \le I_s - I_{rt})$.

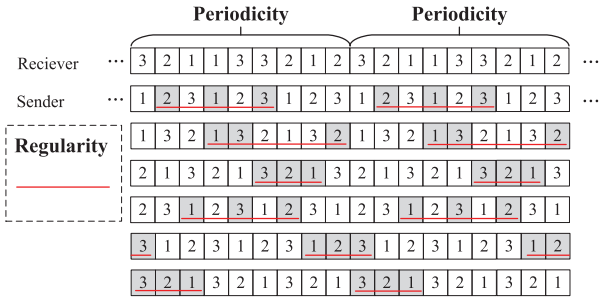

(a) The periodicity and the regularity of ACH

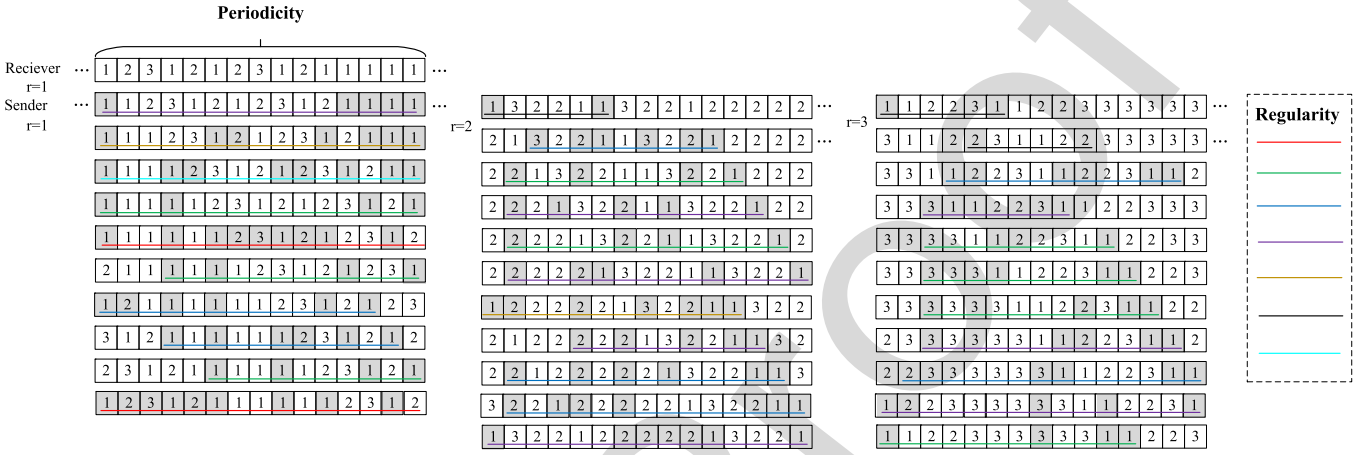

(b) The periodicity and the regularity of JS, r represents step length chosen from (1,M) where M is number of channel

Fig. 8. Examples of rendezvous algorithms.

Since submatrix Q is a strict upper triangular matrix, P^I can be expressed as

$$\mathrm{P}^I = \sum_{k=0}^{\infty} \mathrm{Q}^k = \sum_{k=0}^{I_s - I_{rt}} \mathrm{Q}^k = (\mathrm{I} - \mathrm{Q})^{-1}. \tag{22}$$

In each time slot, an SU always starts from the beginning of the time slot (i.e., the state I_1). Hence, P_{ERI} for CHCS can be expressed as

$$P_{ERI}^{cs}(\varepsilon, T_{ss}, T_{tr}^{cs}) = \left(\mathrm{P}^I \mathrm{R}\right)_{11} = \sum_{j=1}^{I_s - I_{rt}} \left(\mathrm{P}^I\right)_{1j} \cdot p_{st}. \tag{23}$$

Then, $\overline{\Delta}$ can be expressed as

$$\overline{\Delta} = \sum_{j=1}^{I_s - I_{rt}} j \cdot \left(\mathrm{P}^I\right)_{1j} \cdot p_{st}. \tag{24}$$

V. Analysis of CH-Based Rendezvous

A key condition for SUs to establish a link is to achieve rendezvous. For the sake of analysis, we assume that the PU activity is unchanged during the rendezvous process. Due to the fact that SUs can start a CH rendezvous process in a random time slot, the probabilities that SUs start hopping in time slot i or time slot j are equal. Then, the relationship between $ATTR$ and $ATSR$ is expressed as

$$ATTR = \frac{ATSR + 1}{2}. \tag{25}$$

The A-type CH algorithms (see Section II) have inherent regularity in CH sequences and thus it is easy to derive $ATSR$ of these algorithms. The B-type CH algorithms (see Section II) usually use prime number modular arithmetic to guarantee rendezvous, which can be seen as a circle walk on a clock. However, the ***regularity*** and the ***periodicity*** of these CH algorithms can still be derived via the analysis. The ***regularity*** means that there are several rendezvous patterns in a rendezvous algorithm, and all rendezvous scenarios are contained in these rendezvous patterns. In each pattern, rendezvous always occurs periodically, which is the ***periodicity***. We can employ the ***regularity*** to determine average number of rendezvous slots in a ***periodicity***. To be more specific, different rendezvous patterns of the CH algorithm contain different numbers of rendezvous slots (see Fig. 8). Then, the average number of rendezvous slots in a ***periodicity*** with M channels can be expressed as

$$E\left[R_M\right] = \sum^{\Omega} n_{ren}^i \cdot p_{ren}^i \quad (\forall i,\ i \in \Omega), \tag{26}$$

where n_{ren}^i and p_{ren}^i represent the number of rendezvous slots in $pattern\ i$ and the corresponding proportion respectively, and Ω is set of all rendezvous patterns.

Fig. 8 shows examples of the ***regularity*** and the ***periodicity*** of two typical CH algorithms (i.e., ACH [7] and JS [8]), where there are 3 channels and time slots with the same underline color belonging to same ***regularity***. Because of the limited space, we do not present detailed analysis of these algorithms.

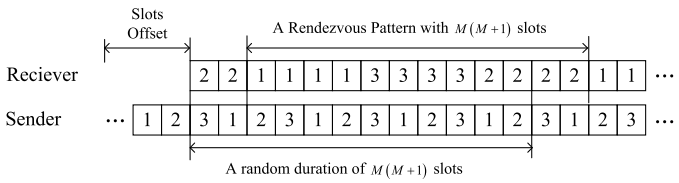

Fig. 9. Illustration of the rendezvous pattern.

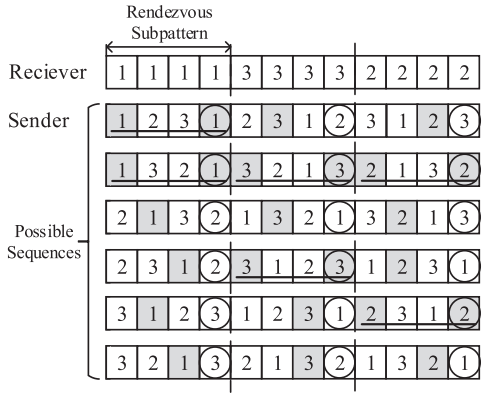

Fig. 10. Examples of rendezvous patterns.

In this paper we take recent Sender Jump-Receiver Wait (SJ-RW) [9] as an example to analyze the $ATSR$ due to its outstanding performance, which can represent the recent advance in this area. In SJ-RW algorithm, the period of the rendezvous pattern is $M(M+1)$ time slots. Every overlap of $M(M+1)$ time slots between any pairwise sequences (i.e., a sender's and a receiver's sequences) is equal to a rendezvous pattern with $M(M+1)$ time slots (see Fig. 9 and refer to [9] for more details).

In SJ-RW, the sender stays on a channel for a time slot while the receiver for $M+1$ time slots. Hence, the sender repeats visiting one channel after visiting all channels when the receiver waits on the channel for $M+1$ time slots, which represents a rendezvous subpattern. More specifically, this indicates that if the repeating channel is the same channel that the receiver waits on, then during these $M+1$ time slots there exist two rendezvous slots; we call this rendezvous subpattern as *Two-Rendezvous Subpattern* (see underlined successive time slots in Fig. 10), and the others *One-Rendezvous Subpattern*. Furthermore, if channel-visiting order of sender is the same with that of the receiver, then there will be M Two-Rendezvous Subpatterns and in total $2M$ rendezvous slots in a rendezvous pattern (see the second sequence in Fig. 10, i.e., there are 3 Two-Rendezvous Subpatterns in this rendezvous pattern).

We can determine that for a specific channel, if the sender's channel-visit order of this channel is the same as the receiver's, the Two-Rendezvous Subpattern occurs; otherwise, the One-Rendezvous Subpattern occurs. Furthermore, we can conclude that permutations and combinations of Two-Rendezvous Subpatterns and One-Rendezvous Subpatterns are equivalent to the differences between sender's and receiver's channel-visit orders. This can be modeled as the Derangement Problem in Discrete Mathematics [28]. We refer to the same channel that the sender and receiver visit in a different order as the *derangement channel*. According to the principle of inclusion-exclusion, the number of patterns with k derangement channels $D(k)$ can be expressed as

$$D(k) = k!\left(\sum_{r=2}^{k}(-1)^r\frac{1}{r!}\right) \quad (k \geq 2). \tag{27}$$

$E[R_M]$ can be derived as

$$E[R_M] = \sum_{d=2}^{M}(2M-d)\cdot\frac{\mathrm{C}_M^d \cdot D(d)}{M!} + \frac{2}{(M-1)!}, \tag{28}$$

where d is the number of the derangement channels. Then, $ATSR$ can be expressed as

$$ATSR = \frac{M(M+1) - E[R_M]}{E[R_M]}. \tag{29}$$

From a long run of CH process, P_{ren} can be derived as

$$P_{ren} = \frac{1}{ATSR+1}. \tag{30}$$

Thus, we now get closed-form expressions of $ATTR$ and $ATSR$ to further formulate access delay for CHCS and CHNCS.

VI. Optimization Models and Algorithms

The objective is to minimize access delays of both CHNCS and CHCS by jointly optimizing ε and T_{ss}, using the proposed access delay model. In order to easily obtain optimized parameters in online applications, a Bio-inspired Fast Search (BFS) algorithm for CHNCS and a Step-length Adaptation based Fast Search (SAFS) algorithm for CHCS are proposed to search for the optimal parameters and calculate the corresponding minimum access delay, respectively.

A. Interference Probability Constraint

In order to ensure that PUs have the highest priority to access spectrum, an interference probability threshold is set to protect PUs from SUs' interference in both CHNCS and CHCS scenarios.

Actually, it is possible for SUs' transmissions colliding with PUs' if miss detections occur and at least one SU transmits during T_{tr}. Then, the interference probability can be expressed as

$$P_I(\varepsilon, T_{ss}) = P_b \cdot P_m(\varepsilon, T_{ss}) \cdot P_{tra} \tag{31}$$

where P_{tra} is the conditional probability that at least one SU transmits during T_{tr}, given that the channel is sensed idle.

B. Optimization for CHNCS

For CHNCS, due to Eq. (14), P_{tra} in Eq. (31) can be expressed as

$$P_{tra}^{ncs} = 1. \tag{32}$$

Then, $P_I(\varepsilon, T_{ss})$ can be expressed as

$$P_I^{ncs}(\varepsilon, T_{ss}) = P_b \cdot P_m(\varepsilon, T_{ss}). \tag{33}$$

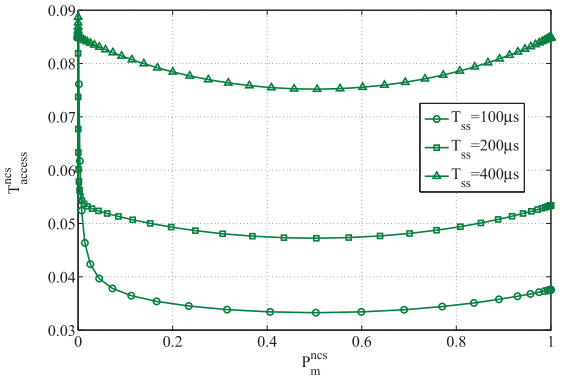

Fig. 11. P_m^{ncs} vs. T_{access}^{ncs} in varied T_{ss}.

The optimization model on the access delay can be formulated as

$$\underset{\varepsilon, T_{ss},}{\text{minimize}} \ \overline{T_{AD}^{ncs}}$$
$$\text{subject to } P_I^{ncs}(\varepsilon, T_{ss}) \le \bar{P}_I, \tag{34}$$

We run extensive simulations (i.e., exhaustive search on T_{ss}^{ncs}) to minimize T_{access}^{ncs}; we found that the relation between P_m^{ncs} and T_{access}^{ncs} may not be monotone. For example, Fig. 11 shows that T_{access}^{ncs} first deceases and increases with increasing P_m^{ncs}. That is to say, for a given T_{ss}^{ncs} and $\bar{P}_I$, the optimal ε_{opt}^{ncs} may satisfy $P_I^{ncs}(\varepsilon_{opt}^{ncs}, T_{ss}^{ncs}) < \bar{P}_I$. Then, we use Firefly Algorithm [13] to develop a Bio-inspired Fast Search (BFS) algorithm to search for the optimal ε and T_{ss}. **Algorithm 1** shows the pseudo-code of the algorithm.

In **Algorithm 1**, F_{access}^{ncs} is the formulation of access delay which can be obtained using Eqs. (5)–(7), (13) and (15). $\mathrm{Rand}(1)$ is the function that generates float number within (0,1). Light is the array of light intensity value of all fireflies, in ascending order. Lines 6-10 indicate that firefly i with smaller light intensity moves towards firefly j with larger light intensity and the step length is restrained by α, β and θ, which represent randomness factor, directional strength and absorption coefficient respectively. Lines 11-14 make sure that each firefly moves within the search range. Line 16 accelerates convergence of the firefly algorithm.

C. Optimization for CHCS

For CHCS, during T_{tr}^{cs} there exist I_s backoff slots; let $\hat{P}_{tra}$ represent the probability that at least one SU transmits in a backoff slot. P_{tra} can be expressed as

$$P_{tra}^{cs} = 1 - \left(1 - \hat{P}_{tra}\right)^{I_s}, \tag{35}$$

where $\hat{P}_{tra}$ can be expressed as

$$\hat{P}_{tra} = 1 - (1 - \tau^{cs}) \cdot \sum_{n_s=0}^{N-1} P(n_s) \cdot (1 - \tau^{cs})^{n_s}. \tag{36}$$

Then, $P_I(\varepsilon, T_{ss})$ can be expressed as

$$P_I^{cs}(\varepsilon, T_{ss}) = P_b \cdot P_m(\varepsilon, T_{ss}) \cdot P_{tra}^{cs}. \tag{37}$$

Algorithm 1 : BFS Algorithm for CHNCS

1: **Input**: number of fireflies N_F, maximum number of iterations I^{Max}, search range of T_{ss} (from T_{ss}^{min} to T_{ss}^{max}).
2: Scaling of search range: $S_R = |T_{ss}^{min} - T_{ss}^{max}|$
3: Initialize positions of N_F fireflies: $T_{ss}^i = \mathrm{Rand}(1) \cdot S_R$ and $\varepsilon^i = \mathrm{Rand}(1) \cdot \bar{\varepsilon}(T_{ss}^i)$[3]
4: **for** $I = 1 : MaxI$ **do**
5: Update Light Intensity $Light^i$ of each firefly: $Light^i = 1/F_{access}^{ncs}(\varepsilon^i, T_{ss}^i)$
6: **if** $Light^i < Light^j$ **then**
7: $r = \sqrt{(T_{ss}^i - T_{ss}^j)^2 + (\varepsilon^i - \varepsilon^j)^2}$.
8: $\beta = (1 - \beta_{\min}) \cdot \exp(-\theta r^2) + \beta_{\min}$.
9: $T_{ss}^i = T_{ss}^i(1-\beta) + T_{ss}^j\beta + \alpha(\mathrm{Rand}(1) - 0.5) \cdot S_R$.
10: $\varepsilon^i = \varepsilon^i(1-\beta) + \varepsilon^j\beta + \alpha(\mathrm{Rand}(1) - 0.5) \cdot \bar{\varepsilon}(T_{ss}^i)$.
11: **if** $T_{ss}^i \le T_{ss}^{min}$ **then** $T_{ss}^i = T_{ss}^{min}$ **end if**
12: **if** $T_{ss}^i \ge T_{ss}^{max}$ **then** $T_{ss}^i = T_{ss}^{max}$ **end if**
13: **if** $\varepsilon^i \le 0$ **then** $\varepsilon^i = 0$ **end if**
14: **if** $T_{ss}^i \ge \bar{\varepsilon}(T_{ss}^i)$ **then** $\varepsilon^i = \bar{\varepsilon}(T_{ss}^i)$ **end if**
15: **end if**
16: $\alpha = (\frac{10^{-3}}{9})^{\frac{1}{MaxI}} \cdot \alpha$ //reduce randomness
17: $[\mathrm{Light}, \mathrm{Index}] = \mathrm{Sort}([\mathrm{Light}^1, \ldots, \mathrm{Light}^{N_F}])$
18: **end for**
19: $T_{ss} = T_{ss}(Index)$ and $\varepsilon = \varepsilon(Index)$
20: $T_{ss}^{opt} = T_{ss}^{N_F}$, $\varepsilon^{opt} = \varepsilon^{N_F}$ and $T_{access}^{min} = 1/Light^{N_F}$
21: **Output**: the optimal T_{ss} is T_{ss}^{opt}, the optimal ε is ε^{opt} and the minimum T_{access} is T_{access}^{min}.

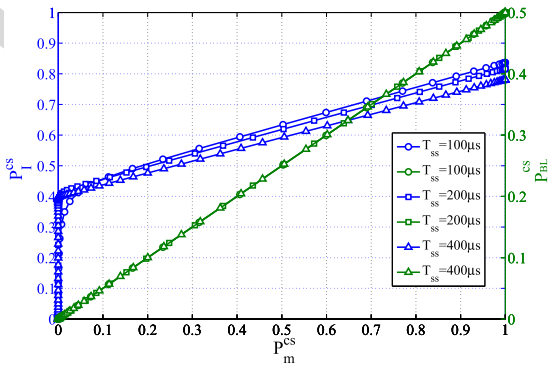

Fig. 12. P_m^{cs} vs. P_I^{cs} in varied T_{ss}.

The optimization model on access delay can be formulated as

$$\underset{\varepsilon, T_{ss},}{\text{minimize}} \ \overline{T_{AC}^{cs}}$$
$$\text{subject to } P_I^{cs}(\varepsilon, T_{ss}) \le \bar{P}_I. \tag{38}$$

According to Eqs. (4) and (35)–(37), P_I^{cs} is an increasing function of P_m^{cs} (see Fig. 12). P_{BL}^{cs} is also monotonically increasing with respect to P_m^{cs} (see Fig. 12). Besides, larger ε results in larger P_m^{cs} due to the fact that P_m^{cs} is an increasing

[3] $\bar{\varepsilon}(T_{ss})$ is the function of upper limit of ε that satisfy $P_I^{ncs}(\varepsilon, T_{ss}) \le \bar{P}_I$ for given T_{ss}, which is $\mathrm{erfcinv}(1 - \frac{\bar{P}_I}{P_b}) \cdot 2\sqrt{f_s T_{ss}(1+2\gamma)} + f_s T_{ss}(1+\gamma)$ where $\mathrm{erfcinv}(\cdot)$ is the inverse function of complementary error function.

Algorithm 2 : SAFS Algorithm for CHCS

1: **Input**: regular search step length S_{reg}, minimum search step length S_{min}, initial searching point T_{ss}^{ini}, end search point T_{ss}^{end}.
2: Initialize access delay T_{access}^{0} for the given T_{ss}^{ini} according to $F_{access}^{cs}(T_{ss})$.
3: **while** $T_{ss}^{i} < T_{ss}^{end}$[4] **do**
4: $T_{ss}^{i} = T_{ss}^{i-1} + \Gamma(\lambda) S_{reg}$.[5]
5: Update T_{access}^{i} with T_{ss}^{i} according to $F_{access}^{cs}(T_{ss})$
6: $\lambda^{i} = (T_{access}^{i} - T_{access}^{i-1})/(T_{ss}^{i} - T_{ss}^{i-1})$
7: **if** $\lambda^{i} \cdot \lambda^{i-1} \leq 0$ **then**
8: **for** $T_{ss}^{j} = T_{ss}^{i-2} : S_{min} : T_{ss}^{i}$ **do**
9: Update T_{access}^{j} with T_{ss}^{j} according to $F_{access}^{cs}(T_{ss})$
10: **if** $T_{access}^{j} \leq T_{access}^{j-1}$ **then**
11: $T_{access}^{min} = T_{access}^{j}$, $T_{ss}^{opt} = T_{ss}^{j}$
12: **end if**
13: **end for**
14: **end if**
15: **end while**
16: **Output**: the optimal T_{ss} is T_{ss}^{opt} and the minimum T_{access} is T_{access}^{min}.

function of ε according to Eqs. (3) and (4). Hence, we have the following corollary:

Corollary 1: The optimal values of ε and T_{ss}, which satisfy $P_I^{cs}(\varepsilon, T_{ss}) \leq \bar{P}_I$ and minimize the access delay T_{access}^{cs} are given by $(\varepsilon^*, T_{ss}^*)$, where $P_I^{cs}(\varepsilon^*, T_{ss}^*) = \bar{P}_I$.

Proof: If we assume that the optimal values of ε and T_{ss} exist such that $P_I^{cs}(\varepsilon^*, T_{ss}^*) < \bar{P}_I$, and there exists a ε^0, such that $\varepsilon^0 > \varepsilon^*$, then, we will have $P_I^{cs}(\varepsilon^0, T_{ss}^*) > P_I^{cs}(\varepsilon^*, T_{ss}^*)$ and $P_m^{cs}(\varepsilon^0, T_{ss}^*) > P_m^{cs}(\varepsilon^*, T_{ss}^*)$ resulting in $P_{BL}^{cs}(\varepsilon^0, T_{ss}^*) > P_{BL}^{cs}(\varepsilon^*, T_{ss}^*)$. Hence, we can conclude that for any given T_{ss}, the optimal ε^{opt} must satisfy $P_I^{cs}(\varepsilon^{opt}, T_{ss}) = \bar{P}_I$ ■

Using Corollary 1, we can reduce the search space of (ε, T_{ss}), and thus the search complexity, by converting a two-dimension solution space to one-dimension solution space. Then, we develop a Step-length Adaptation based Fast Search (SAFS) algorithm, to search for the optimal parameter T_{ss}^{opt} and calculate the corresponding minimum T_{access}^{min}. **Algorithm 2** shows the pseudo-code of the algorithm.

In **Algorithm 2**, $F_{access}^{cs}(T_{ss})$ is the formulation of access delay function which can be obtained using Eqs. (5), (6), (8), (23) and (24). $\Gamma(\lambda)$ is a function for adjusting step length of the search and is equal to $\Gamma(\lambda) = \frac{\mathrm{e}}{1+\mathrm{e}^{-\lambda^2}} - 0.65$ where e is Euler Number; S_{reg} and S_{min} are $25\mu s$ and $2\mu s$, respectively. Line 4 indicates that λ is the slope of at least one point between two adjacent step points (e.g., T_{ss}^{i} and T_{ss}^{i-1}) on the curve of $F_{access}^{cs}(T_{ss})$ according to Lagrange Mean Value Theorem. Line 5 indicates that there is at least one minimum value of T_{access} in $[T_{ss}^{i-2}, T_{ss}^{i}]$ (i.e., where the adjacent slopes are neither positive nor negative). Then, in $[T_{ss}^{i-2}, T_{ss}^{i}]$, exhaustive search on parameter T_{ss}, is used to counteract the possibility of missing optimal value using the non-exhaustive search.

[4] $T_{ss}^{i=0}$ represents T_{ss}^{ini}.
[5] λ is initialized to 0.1 at the beginning.

TABLE II
SIMULATION PARAMETER AND VALUE

Parameter	Value	Parameter	Value
Channel bandwidth	4 MHz	PUs' SNR received by SUs	-7 db
Transmission rate	2 Mbps	Interference probability threshold	5 %
Data length of CTS	128 bit	SIFS for CHCS	10 μs
Data length of RTS	128 bit	DIFS for CHCS	50 μs
Backoff slot	20 μs	Duration of time slot for CHCS	2 ms

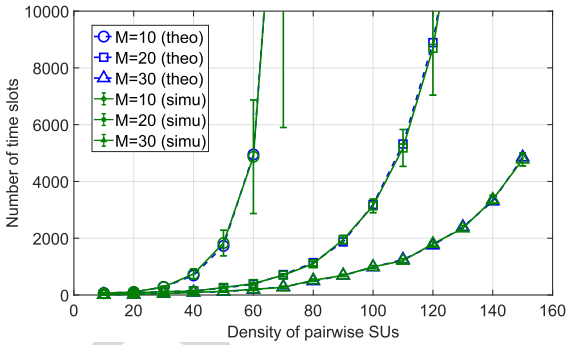

Fig. 13. Verification of access delay model for CHNCS with criteria of time slot.

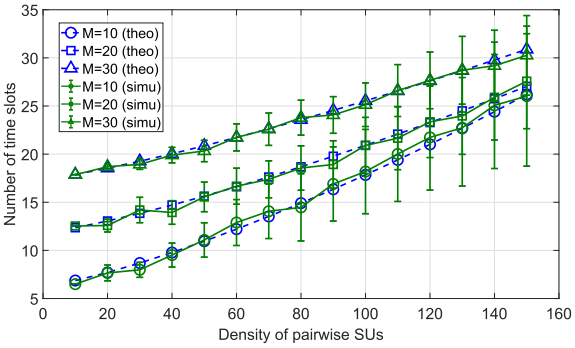

Fig. 14. Verification of access delay model for CHCS with criteria of time slot.

VII. SIMULATION AND ANALYSIS

In this section, the proposed model is validated and the impact of spectrum sensing and multi-SU contention on access delay is analyzed through extensive simulations. In simulations, all SUs are randomly deployed within a space of 100m $\times$ 100m, and each SU has a transmission range of 150m. The P_i and P_b are both 0.5. The experimental results are mean values from 150 independent simulations. Other simulation parameters are listed in Table II.

A. Validation of Theoretical Model

In this subsection, we validate the rendezvous formulation and multi-SU contention model in terms of time slots taken for successfully establishing communication links, for both CHNCS and CHCS without considering PUs' activities. In simulations, SUs can hop on and try to establish links on all channels (i.e., P_{CSI} is equal to 1 for every channel in the theoretical model). The results are shown in Fig. 13 for CHNCS and Fig. 14 for CHCS. The theoretical results perfectly match simulation results in Fig. 13 while

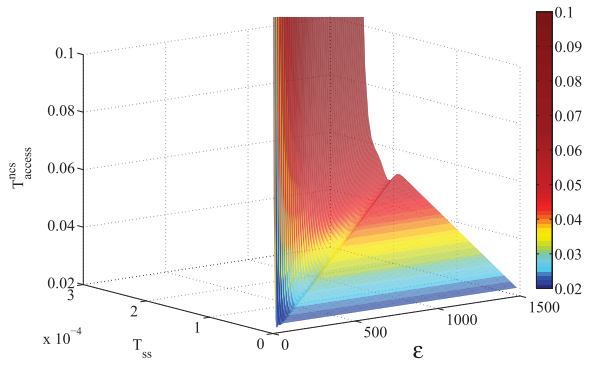

Fig. 15. Access delay jointly impacted by sensing duration and detection threshold in CHNCS scenario.

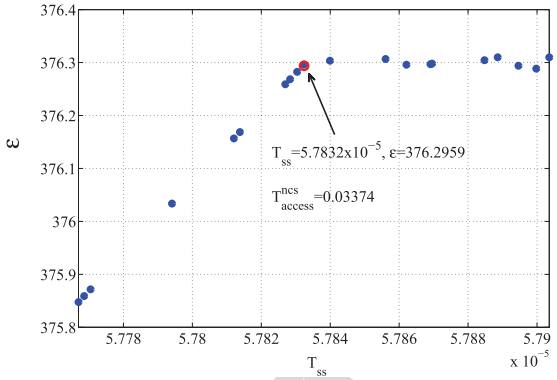

Fig. 16. Result of BFS algorithm under $M = 10$ and $N = 20$.

there are some slight differences between theoretical results and simulation results at some data points in Fig. 14. The reason is that, for CHNCS, the only impacting factor on time slots taken for successfully establishing communication links is the random time and channel of starting CH sequence, while for CHCS, another impacting factor is DCF in multi-SU contention (i.e., randomly selecting number of backoff slots). The impacts (i.e., randomly starting CH sequence and randomly selecting number of backoff slots) on number of time slots are also shown by error bar in Figs. 13 and 14.

Specifically, as shown in Fig. 13, the number of time slots consumed increases exponentially when density of pairwise SUs is increased from 10 to 150 with $M = 10$, 20 and 30. The reason is that larger number of SUs causing more collisions which leads to much more time slots to establish links. Moreover, the standard deviation (i.e., range of error bar) increases with increasing density of pairwise SUs but decreases with increasing number of channels. This is because more collisions caused by larger number of SUs leads to much patterns of establishing links. For example, pairwise SUs may take either 7000 time slots or 3000 time slots to establish a link for $M = 10$ and $N = 60$. However, when the number of channels increases, which results in reducing average number of SUs on each channel, the collisions can be relieved; thus, standard deviation decreases.

In Fig. 14, the relationship between the number of time slots and density of pairwise SUs shows basically linear with $M = 10$, 20 and 30. This can be explained by the fact that CS like DCF based CSMA/CA can further avoid collisions caused by large number of SUs on the same channel. This can be also reflected by the variation of the standard deviation which is smaller than that in Fig. 13.

Statistically, the access delay formulations of both CHNCS and CHCS can well model SU's characteristics in distributed CH-based CRNs.

B. Validation of Proposed Algorithms

The objective in this subsection is to validate the proposed algorithms. We run simulations in the scenario where $M = 10$ and $N = 20$.

Fig. 15 shows a 3-D plot of T^{ncs}_{access} varying with T_{ss} and ε, to reflect joint effects of sensing duration and detection threshold on access delay in CHNCS scenario, without considering the interference probability constraint. In Fig. 15, T_{ss} increases from $5\mu s$ to $300\mu s$ with interval of $5\mu s$, and ε increases from 5 to 1500 with interval of 5. For fixed ε, T^{ncs}_{access} first increases and then decreases and finally increases sharply with increasing T_{ss}. The difference of trends of T^{ncs}_{access} varying with ε for fixed T_{ss} is that T^{ncs}_{access} finally tends to be stable. We observe that the optimal parameters are restricted by the interference probability constraint stated in Eq. (41). Without the interference probability constraint, the optimal T_{ss} and ε both tend to 0. This indicates that, without considering PUs, SUs try to access every channel instead of operating spectrum sensing.

Fig. 16 shows the result derived from BFS algorithm under the configuration that the number of firefly is 20 and the number of iterations is 30, with the constraint that P_I is 5%. The parameters' values used in the simulation are that, β_{min} is 0.4, θ is 1 and α is 0.38. The best 'firefly' circled with red line represents that the obtained optimal T_{ss} is $57.8\mu s$, optimal ε is 376.3 and minimum T^{ncs}_{access} is $33.74ms$; the corresponding probability of detection is 90% and the corresponding probability of false detection is 13.3%.

To validate effectiveness of proposed algorithms in achieving optimal parameters and calculating minimum access delay, we compare BFS algorithm with Grid Search algorithm in terms of obtainable minimum T^{ncs}_{access}, using different computational quantities for CHNCS. We also compare SAFS with Exhaustive Search algorithm in terms of computational quantity, to obtain minimum T^{cs}_{access} for CHCS. Specifically, Grid Search is defined as that, the search is operated on T_{ss} varied from $5\mu s$ to $t_{ss}\mu s$ $(5 < t_{ss} \leq 5n, n = 1, 2, \ldots, 400)$ with interval of $(t_{ss} - 5)/N^{T_{ss}}_{itera}$ μs where $N^{T_{ss}}_{itera}$ is the number of iterations that search on T_{ss}. For each value of T_{ss}, the search on ε varies form 5 to $\varepsilon(T_{ss})$[6] with interval of $(\varepsilon(T_{ss}) - 5)/N^{\varepsilon}_{itera}$ where N^{ε}_{itera} is the number of iterations that search on ε. Thus, the computational quantity of grid search is equal to $N^{T_{ss}}_{itera} \cdot N^{\varepsilon}_{itera}$ and computational quantity of BFS is $N_F \cdot I^{Max}$ (referring to **Algorithm 1**). Exhaustive

[6] $\varepsilon(T_{ss}) = 2\mathrm{erfc}^{-1}(2 - \frac{2\bar{P}_I}{P_b})\sqrt{f_s T_{ss}(1+2\gamma)} + f_s T_{ss}(1+\gamma)$, which indicates that the search is operated under the interference probability constraint.

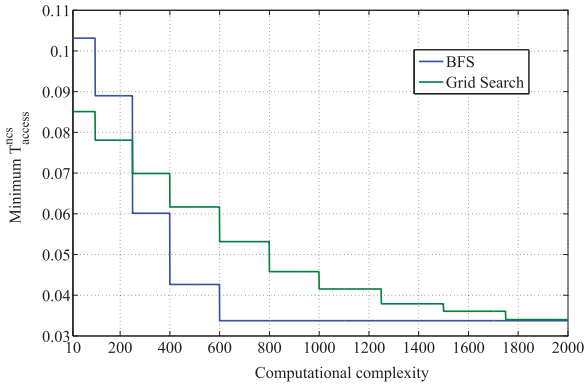

Fig. 17. BFS vs. grid search with different computational quantities.

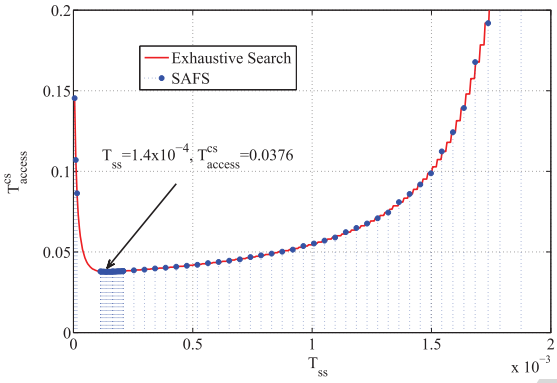

Fig. 18. Comparison between SAFS and exhaustive search in terms of minimum T^{cs}_{access}.

Search is the search operation that is executed on T_{ss} varied from $5\mu s$ to T_{slot} with interval of $5\mu s$ in CHCS scenario.

Fig. 17 shows the obtainable minimum T^{ncs}_{access} with different computational quantities when respectively using BFS and Grid Search. In Fig. 17, it shows that BFS consumes much less calculation (600 iterations of calculation) to get the optimal result than that of Grid Search (approximately 1750 iterations of calculation). The results of comparing SAFS with Exhaustive Search are shown in Fig. 18, where there are 20 SUs and 10 channels; the regular search step length and the minimum search step length in simulation are 25μs and 5μs respectively. In Fig. 18, each blue point with dotted line represents each calculation. Due to the fact that SAFS is able to neglect most redundant calculations, SAFS can save much calculation resource as well as take less time to obtain the optimal parameters and minimum access delay in the CHCS scenario. From Fig. 18, one can observe that the optimal T^{cs}_{ss} is 1.4×10^{-4}s and the corresponding T^{cs}_{access} is 0.0376s; the probability of detection and probability of false detection computed from the obtained optimal parameters are 90% and 0.5% respectively.

C. Performance Analysis

In this subsection, the objective is to analyze cost and benefit of CHNCS over CHCS with optimal parameters (i.e., T_{ss} and ε), in terms of minimum access delay and efficiency of establishing communication links.

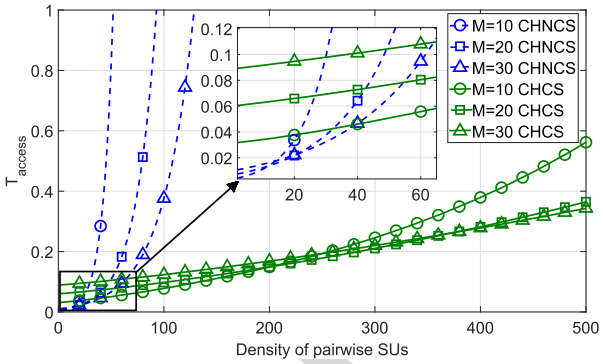

Fig. 19. Access delay performance in different scenarios.

Fig. 19 shows the minimum access delay obtained from the proposed BFS and SAFS algorithms with different density of pairwise SUs. In Fig. 19, as the density of pairwise SUs increases, access delay of both CHNCS and CHCS increases. Besides, access delay of CHNCS increases much more sharply than that of CHCS when the density of pairwise SUs increases. This can be explained by the fact that CHCS allows multiple SU senders to transmit within a time slot with CS like DCF based CSMA/CA, while CHNCS only allows one SU sender to transmit in a time slot. This indicates that, SUs in the CHCS scenario are likely to have more than one opportunity to establish links in the current time slot while SUs in the CHNCS scenario only have one opportunity. Moreover, each failed transmission causes an extra $ATSR$ time slots to achieve another rendezvous. However, it is not always effective to employ CS in CH-based distributed CRNs. In Fig. 19, it shows that access delay of CHNCS is smaller than that of CHCS when the density of pairwise SUs is small (e.g., the density of pairwise SUs is smaller than approximately 20 for $M = 10$). Furthermore, for CHNCS, access delay for $M = 10$ is larger than that for $M = 20$ when the density of pairwise SUs is larger than approximately 10. This can be explained by the fact that when density of pairwise SUs exceeds a threshold (e.g., 10 for comparing $M = 10$ and 20), multi-SU contention (i.e., P_c) impacts more on access delay than CH-based rendezvous (i.e., P_{ren} and $ATSR$). This can also explain the results of comparing $M = 10$ with 30 (threshold of density of pairwise SUs is approximately 15) and $M = 20$ with 30 (threshold of density of pairwise SUs is approximately 20). However, this 'threshold' is much larger for CHCS, e.g., for comparing $M = 10$ with 20 the threshold is approximately 200. The reason is that CS employed in the CHCS scenario can avoid contention and reduce collisions. Thus, the density of pairwise SUs needs to be large enough to reach the intensity of contention when multi-SU impacts more on access delay than CH based rendezvous.

Note that we aim to evaluate the efficiency of establishing communication links in distributed CRNs by the CH scheme. Indeed, in distributed CRNs without a central controller or a CCC, the most important step as well as the first step is to establish a link. Hence, we use communication establishing link rate (CLBR) defined as the number of communication links built by pairwise SUs per second to evaluate the

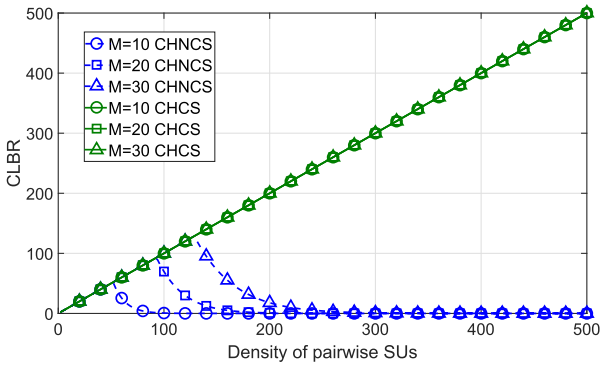

Fig. 20. CLBR performance in different scenarios.

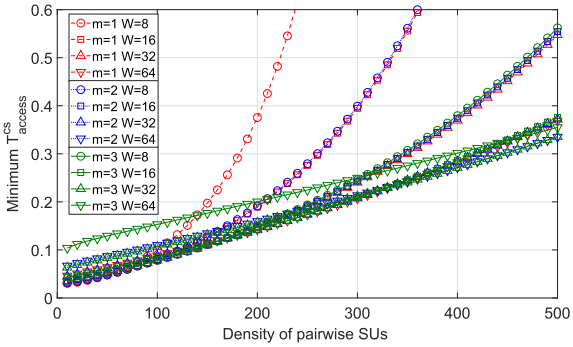

Fig. 21. Minimum access delay performance with different m and W in $M = 10$ scenario.

efficiency performance of CHNCS and CHCS. Specifically, CLBR can be calculated by

$$\text{CLBR} = \begin{cases} \dfrac{N_p}{\overline{T_{AD}}}, & \overline{T_{AD}} > 1 \\ N_p, & \text{otherwise} \end{cases}$$

where N_p is the number of pairwise SUs (i.e., density of pairwise SUs). Fig. 20 shows the performance of CLBR for both CHNCS and CHCS with increasing density of pairwise SUs. In Fig. 20, CLBR for CHNCS first increase, and then decreases as density of pairwise SUs increases from 2 to 500. However, CLBR for CHCS always increases. This can also be explained by the fact that CS allows multiple SUs to transmit in a time slot. Besides, for CHNCS, when the number of channels is larger in CRNs, the CLBR is larger with increasing density of pairwise SUs. This is because larger number of channels can ease the contention of SUs on each channel.

From Figs. 19 and 20, we can conclude that when there exist small number of SUs, it is better to not use CS in CH-based distributed CRNs.

D. Impact Analysis of MAC Parameters

The objective is to evaluate the impacts of MAC parameters (i.e., m and W) on minimum access delay for CHCS. Figs. 21 and 22 show the minimum T^{cs}_{access} varies with density of pairwise SUs in different scenarios. In the scenario that $M = 10$ in Fig. 21, the minimum T^{cs}_{access} with smaller m and W increases faster when the density of pairwise SUs increases. Although the minimum T^{cs}_{access} with smaller m and W is smaller when density of pairwise SUs is small

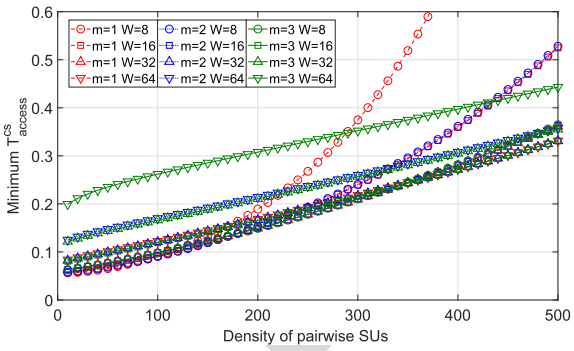

Fig. 22. Minimum access delay performance with different m and W in $M = 20$ scenario.

(e.g., approximately 140 for $m = 1$ and $W = 8$ comparing with $m = 3$ and $W = 64$), it is finally larger than that with larger m and W with increasing density of pairwise SUs. However, in the scenario that $M = 20$ in Fig. 22, the minimum T^{cs}_{access} with larger m and W is much larger than that with smaller m and W when density of pairwise SUs is small (e.g., approximately 280 for $m = 1$ and $W = 8$ comparing with $m = 3$ and $W = 64$). This can be explained as follows. When the number of SUs on each channel is small, the CH-based rendezvous impacts more than multi-SU contention, but CH-based rendezvous impacts less than multi-SU contention when the number of SUs on each channel is large.

VIII. Conclusion

This paper proposes a tradeoff problem between spectrum sensing duration and time slot duration for CHNCS and a tradeoff problem between spectrum sensing duration and contention transmission duration for CHCS, in distributed CRNs from a cross-layer perspective. For both scenarios, imperfect spectrum sensing in PHY layer and CH-based rendezvous in MAC layer are jointly taken into consideration. Specifically, we first derive the exact expressions of the probability that SUs access channels being aware of the impact of imperfect spectrum sensing. Then, by jointly considering the impact of imperfect spectrum sensing and CH-based rendezvous algorithm, we employ an absorbing Markov chain to model the multi-SU contention transmission process for CHCS and derive the probability of SUs successfully exchanging rendezvous information for both scenarios. Furthermore, we formulate the corresponding access delay models for both CHNCS and CHCS with the constraint of interference probability to protect PUs' activities. Finally, we propose a bio-inspired algorithm to search for the optimal parameters (i.e., sensing duration and detection threshold) for CHNCS and propose a self-adaptive step length algorithm to search for the optimal sensing duration for CHCS. Numerical simulation results show that (i) the theoretical results obtained from access delay models for CHNCS and CHCS both match simulation results well, which indicates that the access delay models for both scenarios well simulate SUs establishing communication link in distributed CRNs; (ii) both BFS algorithm and SAFS algorithm can effectively obtain the optimal parameters of minimum access delay with consuming less computational resource; (iii) in terms of access delay,

when there exist fewer SUs (e.g., 20 for $M = 10$) the access delay of CHNCS is smaller than that of CHCS. However, when the number of SUs increases, the access delay of CHNCS increases more rapidly than that of CHCS. Besides, it can be concluded that with the number of SUs increasing multi-SU contention impacts more than CH based rendezvous on access delay; (iv) in term of CLBR, due to the intense collisions caused by increasing SUs, CLBR of CHNCS has worse performance than that of CHNCS; (v) similarly in conventional IEEE 802.11 DCF based wireless networks, proper values of m and W can effectively avoid the contention and collision caused by large number of SUs.

REFERENCES

[1] N. C. Theis, R. W. Thomas, and L. A. DaSilva, "Rendezvous for cognitive radios," *IEEE Trans. Mobile Comput.*, vol. 10, no. 2, pp. 216–227, Feb. 2011.

[2] P. M. R. dos Santos, M. A. Kalil, O. Artemenko, A. Lavrenko, and A. Mitschele-Thiel, "Self-organized common control channel design for cognitive radio ad hoc networks," in *Proc. IEEE PIMRC*, Sep. 2013, pp. 2419–2423.

[3] K. G. M. Thilina, E. Hossain, and D. I. Kim, "DCCC-MAC: A dynamic common-control-channel-based MAC protocol for cellular cognitive radio networks," *IEEE Trans. Veh. Technol.*, vol. 65, no. 5, pp. 3597–3613, May 2016.

[4] A. M. Masri, C. F. Chiasserini, C. Casetti, and A. Perotti, "Common control channel allocation in cognitive radio networks through UWB communication," *J. Commun. Netw.*, vol. 14, no. 6, pp. 710–718, Dec. 2012.

[5] X. J. Tan, C. Zhou, and J. Chen, "Symmetric channel hopping for blind rendezvous in cognitive radio networks based on union of disjoint difference sets," *IEEE Trans. Veh. Technol.*, vol. 66, no. 11, pp. 10233–10248, Nov. 2017.

[6] R. Paul and Y.-J. Choi, "Adaptive rendezvous for heterogeneous channel environments in cognitive radio networks," *IEEE Trans. Wireless Commun.*, vol. 15, no. 11, pp. 7753–7765, Nov. 2016.

[7] K. Bian and J.-M. Park, "Maximizing rendezvous diversity in rendezvous protocols for decentralized cognitive radio networks," *IEEE Trans. Mobile Comput.*, vol. 12, no. 7, pp. 1294–1307, Jul. 2013.

[8] H. Liu, Z. Lin, X. Chu, and Y.-W. Leung, "Jump-stay rendezvous algorithm for cognitive radio networks," *IEEE Trans. Parallel Distrib. Syst.*, vol. 23, no. 10, pp. 1867–1881, Oct. 2012.

[9] J. Li, H. Zhao, J. Wei, D. Ma, and L. Zhou, "Sender-jump receiver-wait: A simple blind rendezvous algorithm for distributed cognitive radio networks," *IEEE Trans. Mobile Comput.*, vol. 17, no. 1, pp. 183–196, Jan. 2018.

[10] C.-M. Chao, H.-Y. Fu, and L.-R. Zhang, "A fast rendezvous-guarantee channel hopping protocol for cognitive radio networks," *IEEE Trans. Veh. Technol.*, vol. 64, no. 12, pp. 5804–5816, Dec. 2015.

[11] *Standard for Information Technology—Local and Metropolitan Area Networks - Specific Requirements—Part 22: Cognitive Radio Wireless Regional Area Networks (WRAN) Medium Access Control (MAC) and Physical Layer (PHY) Specifications: Policies and Procedures for Operation in the Bands that Allow Spectrum Sharing where the Communications Devices May Opportunistically Operate in the Spectrum of the Primary Service*, IEEE Standard 802.22, 2011. [Online]. Available: http://grouper.ieee.org/groups/802/22

[12] S. Zhang, A. S. Hafid, H. Zhao, and S. Wang, "Cross-layer rethink on sensing-throughput tradeoff for multi-channel cognitive radio networks," *IEEE Trans. Wireless Commun.*, vol. 15, no. 10, pp. 6883–6897, Oct. 2016.

[13] X.-S. Yang, "Firefly algorithms for multimodal optimization," in *Stochastic Algorithms: Foundations and Applications*. Berlin, Germany: Springer, 2009, pp. 169–178.

[14] S. Wang, J. Zhang, and L. Tong, "A characterization of delay performance of cognitive medium access," *IEEE Trans. Wireless Commun.*, vol. 11, no. 2, pp. 800–809, Feb. 2012.

[15] Z. Liang, S. Feng, D. Zhao, and X. S. Shen, "Delay performance analysis for supporting real-time traffic in a cognitive radio sensor network," *IEEE Trans. Wireless Commun.*, vol. 10, no. 1, pp. 325–335, Jan. 2009.

[16] W. Li, X. Cheng, T. Jing, Y. Cui, K. Xing, and W. Wang, "Spectrum assignment and sharing for delay minimization in multi-hop multi-flow CRNs," *IEEE J. Sel. Areas Commun.*, vol. 31, no. 11, pp. 2483–2493, Nov. 2013.

[17] Q. Liu, X. Wang, B. Han, X. Wang, and X. Zhou, "Access delay of cognitive radio networks based on asynchronous channel-hopping rendezvous and CSMA/CA MAC," *IEEE Trans. Veh. Technol.*, vol. 64, no. 3, pp. 1105–1119, Mar. 2015.

[18] S. E. Safavi and K. P. Subbalakshmi, "Effective bandwidth for delay tolerant secondary user traffic in multi-PU, multi-SU dynamic spectrum access networks," *IEEE Trans. Cogn. Commun. Netw.*, vol. 1, no. 2, pp. 175–184, Jun. 2015.

[19] D. Zhang, T. He, F. Ye, R. K. Ganti, and H. Lei, "Neighbor discovery and rendezvous maintenance with extended quorum systems for mobile applications," *IEEE Trans. Mobile Comput.*, vol. 16, no. 7, pp. 1967–1980, Jul. 2017.

[20] C. de Sousa, D. Passos, R. C. Carrano, and C. V. Albuquerque, "Multichannel continuous rendezvous in cognitive networks," in *Proc. ACM MSWiM*, 2017, pp. 63–70.

[21] X. Liu and J. Xie, "A practical self-adaptive rendezvous protocol in cognitive radio ad hoc networks," in *Proc. IEEE INFOCOM*, Apr./May 2014, pp. 2085–2093.

[22] Y.-C. Liang, Y. Zeng, E. C. Y. Peh, and A. T. Hoang, "Sensing-throughput tradeoff for cognitive radio networks," *IEEE Trans. Wireless Commun.*, vol. 7, no. 4, pp. 1326–1337, Apr. 2008.

[23] M. A. Hossain and N. I. Sarkar, "A distributed multichannel MAC protocol for rendezvous establishment in cognitive radio ad hoc networks," *Ad Hoc Netw.*, vol. 70, pp. 44–60, Mar. 2018.

[24] K. Tan, H. Liu, J. Zhang, Y. Zhang, J. Fang, and G. M. Voelker, "Sora: High-performance software radio using generalpurpose multi-core processors," *Commun. ACM*, vol. 54, no. 1, pp. 99–107, Jan. 2011.

[25] C. Cordeiro, K. Challapali, and D. Birru, "IEEE 802.22: An introduction to the first wireless standard based on cognitive radios," *J. Commun.*, vol. 1, no. 1, pp. 38–47, Apr. 2006.

[26] H. Zhao, K. Ding, N. I. Sarkar, J. Wei, and J. Xiong, "A simple distributed channel allocation algorithm for D2D communication pairs," *IEEE Trans. Veh. Technol.*, vol. 67, no. 11, pp. 10960–10969, Nov. 2018.

[27] X. Liu and J. Xie, "A slot-asynchronous MAC protocol design for blind rendezvous in cognitive radio networks," in *Proc. IEEE Globecom*, Dec. 2014, pp. 4641–4646.

[28] K. H. Rosen, "Counting," in *Discrete Mathematics and Its Applications*, 7th ed. New York, NY, USA: McGraw-Hill, 2012, pp. 407–434.

[29] G. Bianchi, "Performance analysis of the IEEE 802.11 distributed coordination function," *IEEE J. Sel. Areas Commun.*, vol. 18, no. 3, pp. 535–547, Mar. 2000.

[30] D. P. Bertsekas and J. N. Tsitsiklis, "Markov Chains," in *Introduction to Probability*, 2th ed. Nashua, NH, USA: Athena Scientific, 2008, pp. 339–405.

Jiaxun Li received the B.S. and M.S. degrees from the National University of Defense Technology (NUDT), Changsha, China, in 2013 and 2015, respectively, where he is currently pursuing the Ph.D. degree, all in information and communication engineering. He visited the Ph.D. Student at the University of Montreal, Canada, from 2017 to 2018. He has served as a Reviewer for many international journals such as the IEEE SYSTEM JOURNAL, the IEEE COMMUNICATION LETTER, and the *IEEE Communication Magazine*. His main research interests include cognitive radio networks and resource optimization.

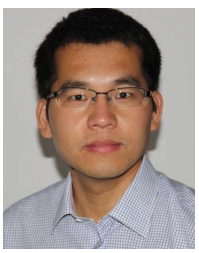

Haitao Zhao (M'13–SM'18) received the M.S. and Ph.D. degrees in information and communication engineering from the National University of Defense Technology (NUDT), Changsha, China, in 2004 and 2009, respectively. He has visited the Institute of Electronics, Communications and Information Technology, Queens University Belfast, U.K., from 2008 to 2009, and conducted post-doctoral research with Hong Kong Baptist University from 2014 to 2015. He is currently a Professor with the College of Electronic Science and Engineering, NUDT. His main research interests include cognitive radio networks, self-organized networks, and cooperative communications. He is currently a member of the ACM, Worldwide University Network Cognitive Communications Consortium, and also a Mentor Member of the IEEE 1900.1 standard. He has served as a TPC Member of the IEEE ICC from 2014 to 2019 and GLOBECOM 2015 to 2019. He has served as a guest editor for several international journal special issues on cognitive radio networks.

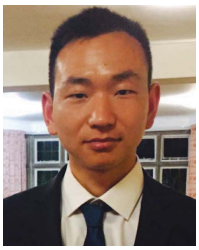

Shaojie Zhang received the M.S. and Ph.D. degrees in information and communication engineering from the National University of Defense Technology, Changsha, China, in 2012 and 2016, respectively. He is currently a Lecturer with the Army Aviation Institute of PLA, Beijing, China. His current research interests include cognitive radio networks and performance analysis and optimization.

Abdelhakim Senhaji Hafid was a Senior Research Scientist with Bell Communications Research (Bellcore), NJ, USA, where he spent several years focusing on the context of major research projects on the management of next generation networks. He is currently a Full Professor with the University of Montreal. He is also the Founding Director of the Network Research Laboratory and the Montreal Blockchain Laboratory. He is a Research Fellow of CIRRELT, Montreal, Canada. He has extensive academic and industrial research experience in the areas of management and design of next generation networks. His current research interests include IoT, fog/edge computing, blockchain, and intelligent transport systems.

Dusit Niyato (M'09–SM'15–F'17) received the B.Eng. degree from the King Mongkuts Institute of Technology Ladkrabang, Thailand, in 1999, and the Ph.D. degree in electrical and computer engineering from the University of Manitoba, Canada, in 2008. He is currently a Professor with the School of Computer Science and Engineering, Nanyang Technological University, Singapore. His research interests are in the areas of energy harvesting for wireless communication, the Internet of Things, and sensor networks.

Jibo Wei received the B.S. and M.S. degrees from the National University of Defense Technology (NUDT), Changsha, China, in 1989 and 1992, respectively, and the Ph.D. degree from Southeast University, Nanjing, China, in 1998, all in electronic engineering. He is currently a Professor with the Department of Communication Engineering, NUDT. His research interests include wireless network protocol and signal processing in communications, cooperative communication, and cognitive network. He is a Member of the IEEE Communication Society and the IEEE VTS. He is a Senior Member of the China Institute of Communications and Electronics. He is also an Editor of the *Journal of China Communications*.

Cross-Layer Analysis and Optimization on Access Delay in Channel-Hopping-Based Distributed Cognitive Radio Networks

Jiaxun Li, Haitao Zhao, *Senior Member, IEEE*, Shaojie Zhang, Abdelhakim Senhaji Hafid, *Member, IEEE*, Dusit Niyato, *Fellow, IEEE*, and Jibo Wei, *Member, IEEE*

***Abstract*— In channel-hopping (CH)-based distributed cognitive radio networks (CRNs), the time duration that secondary users (SUs) spend for establishing communication links is called access delay. To evaluate access delay, we propose an access delay model by jointly considering imperfect spectrum sensing and multi-channel multi-SU transmission, from the cross-layer perspective. The model considers two typical scenarios. The first scenario assumes that the SUs do not use contention scheme (CS) which indicates that the time slot is relatively shorter to just allow a transmission. The second scenario assumes that the SUs employ CS [i.e., modified Distributed Coordination Function (DCF)-based Carrier Sense Multiple Access/Collision Avoidance (CSMA/CA) in this paper], which indicates that the time slot is long enough to regulate multiple transmissions. We then propose a bio-inspired algorithm for the first scenario and a self-adaptive step-length algorithm for the second scenario to search for the optimal values of spectrum sensing parameters. The theoretical analysis and simulation results validate the proposed access delay model and show that the proposed algorithms can reduce the most redundant computation. They also show that the optimization of cross-layer parameters can significantly decrease SUs' access delay. Moreover, we conduct a cost-benefit analysis to evaluate the performance of the two scenarios.**

***Index Terms*— Blind rendezvous, cognitive radio networks, channel-hopping, optimization, spectrum sensing.**

I. Introduction

COGNITIVE radio (CR) has emerged as an advanced and promising technology to exploit wireless spectrum opportunistically. In CRNs, any pair of SUs are required to locate each other on the spectrum to establish a communication link, which is referred to as 'rendezvous' [1]. Typically, employing a dedicated common control channel (CCC) is manageable and effective to exchange rendezvous information. Hence, most early works use CCC [2]–[4] to facilitate the rendezvous process. However, the CCC design may be inflexible or even fragile in highly dynamic networks scenarios, especially in distributed CRNs. Thus, various CH algorithms, which do not rely on any preassigned controller or CCC, have been widely studied to tackle the rendezvous problem in distributed CRNs. In these works [1], [5]–[10], [19]–[21], [26], a sender SU and a receiver SU are described as *Achieve Rendezvous* if they hop on a same channel in the same time slot. The amount of time that they spend for achieving rendezvous is called *Time To Rendezvous* (TTR). Even though CH-based rendezvous schemes can overcome the drawbacks introduced by CCC-based rendezvous schemes, TTR of CH scheme is relatively longer due to the fact that SUs with CH scheme have to hop on and access every available channel for any potential rendezvous [9]. Hence, the key objective in designing CH scheme is to minimize TTR. Most of these designs focus on developing an effective CH sequence [1], [5]–[10], [19], [20], [26]. However, SUs that achieve rendezvous cannot always communicate with each other because of transmission collision caused by multiple SUs hopping on a same channel and transmitting at the same time. In this paper, the time duration taken by a pair of SUs for establishing a communication link (i.e., successfully exchanging rendezvous information) is called access delay. In distributed CRNs, the first step for SUs is to establish communication links with each other. In this sense, access delay is an important metric to evaluate performance of forming distributed CRNs.

Contention scheme (CS) such as Distributed Coordination Function (DCF) based Carrier Sense multiple Access/Collision Avoidance (CSMA/CA), which allows multiple SUs to transmit within the same time slot in a distributed manner, is employed in many works to avoid collision [5]–[10], [17]–[21], [27]. However, in this case, a long enough duration has to be reserved in the time slot for SUs to contend for transmission opportunities. Then, the access delay in CH with CS (CHCS) may be large because it may take SUs

Manuscript received July 22, 2018; revised November 30, 2018 and February 4, 2019; accepted February 18, 2019. This work is supported in part by National Natural Science Foundation of China under grant No. 61471376. The associate editor coordinating the review of this paper and approving it for publication was D. Marabissi. *(Corresponding author: Haitao Zhao.)*

J. Li, H. Zhao, and J. Wei are with the College of Electronic Science and Engineering, National University of Defense Technology, Changsha 410073, China (e-mail: lijiaxun@nudt.edu.cn; haitaozhao@nudt.edu.cn).

S. Zhang is with the Army Aviation Institute of PLA, Beijing 101149, China (e-mail: zhangshaojie@nudt.edu.cn).

A. S. Hafid is with the Department of Computer Science and Operations Research, University of Montreal, Quebec, H3C 3J7, Canada (e-mail: ahafid@iro.umontreal.ca).

D. Niyato is with the School of Computer Science and Engineering, Nanyang Technological University, Singapore 639798, and also with the School of Physical and Mathematical Sciences, Nanyang Technological University, Singapore 639798 (e-mail: dniyato@ntu.edu.sg).

Color versions of one or more of the figures in this paper are available online at http://ieeexplore.ieee.org.

Digital Object Identifier 10.1109/TCOMM.2019.2903112

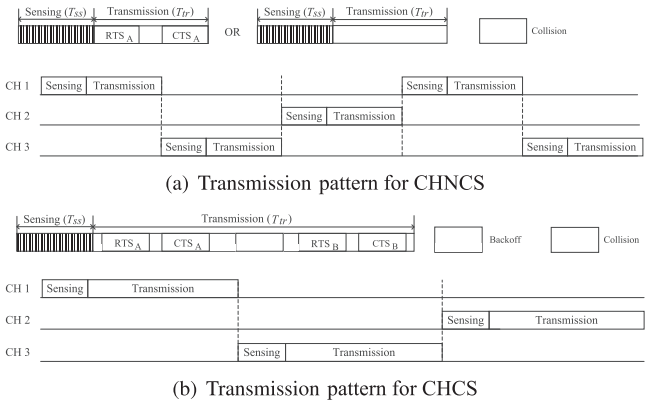

(a) Transmission pattern for CHNCS

(b) Transmission pattern for CHCS

Fig. 1. Transmission patterns for CHCS and CHNCS scenarios.

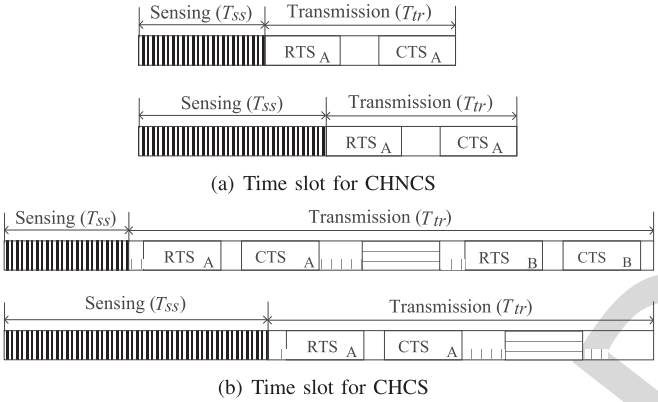

(a) Time slot for CHNCS

(b) Time slot for CHCS

Fig. 2. Structures of time slot with different sensing durations for CHCS and CHNCS.

multiple slots to achieve rendezvous with target SUs. In CH without CS (CHNCS), the time slot can be relatively short for only allowing one transmission of rendezvous information; thus, SUs may establish communication links with smaller access delay. The differences between these two scenarios are depicted in Fig. 1. As depicted in Fig. 1 (a), in CHNCS scenario, the transmission duration of a time slot only contains a RTS/CTS transmission or collision by multi-SU transmission. However, for CHCS in Fig. 2 (b), though there may also exist collisions during transmission duration in the time slot, SUs may still successfully transmit RTS/CTS within the transmission duration; this is because that large transmission duration is reserved to allow multiple transmissions by using CSMA/CA. Comparing Fig. 1 (a) and (b), CHNCS has short duration of time slot but is easy to cause collision while CHCS allows multiple transmissions but has long transmission duration. Hence, impacts of length of time slot and CS in CH on access delay should be analyzed to evaluate the performance of access delay in both CHCS and CHNCS scenarios.

In order to protect primary users' (PU) transmissions, SUs have to perform spectrum sensing to sense PUs' activities on channels and avoid interferences. However, it is likely for SUs to perform imperfect spectrum sensing in practice. Once imperfect spectrum sensing occurs, SUs will either not access an idle channel (false detection) or access a channel that PUs are using (miss detection).

The structures of time slot with different sensing durations for CHCS and CHNCS are shown in Fig. 2. On the one hand,long enough duration of spectrum sensing can provide accurate sensing results that contribute to protect PUs and avoid wasting transmission opportunities in both CHCS and CHNCS. On the other hand, in the case of CHNCS, as shown in Fig. 2 (a), long spectrum sensing time results in long time slot, which may increase access delay; in the case of CHCS, as shown in Fig. 2 (b), long spectrum sensing time results in short contention time whereas multiple SUs should be given long enough time to use CS for exchanging rendezvous information on the rendezvous channel.

In this paper,[1] we formulate the access delay model and propose corresponding optimization algorithms for both CHCS and CHNCS scenarios. The main contributions are as follows.

- We formulate the novel access delay model based on the assumptions that SUs employ CS (i.e., CHCS) and that SUs do not employ CS (i.e., CHNCS) respectively, in CH based rendezvous; the model jointly considers the impacts of imperfect spectrum sensing, specific CH algorithm and multi-SU transmission under the constraint of interference to PUs.
- We propose a methodology to analyze the number of time slots consumed for rendezvous of CH algorithms, and derive closed-form expressions of average number of time slots consumed for the first rendezvous and successive rendezvous.
- We propose a bio-inspired algorithm which employs the firefly algorithm [13] to quickly search the optimal parameters (i.e., sensing duration and detection threshold) for CHNCS; we propose an algorithm which can autonomously adjust step-length for searching optimal parameters (i.e., sensing duration) for CHCS.
- We investigate the benefit and cost of establishing communication links using CHNCS over CHCS in terms of access delay and analyze performance of both CHNCS and CHCS under different scenarios where there exist different number of SUs and channels.

The rest of the paper is organized as follows. Section II reviews related work. Section III describes the system model and outlines the access delay problem. Section IV presents analysis of multi-channel multi-SU access for both CHNCS and CHCS. Section V presents analysis of channel hopping algorithm where Sender Jump-Receiver Wait (SJ-RW) [9] is taken as an example. Section VI presents optimization algorithms on access delay for both CHNCS and CHCS. Section VII presents simulation results and discusses impacts of number of SUs and channels. Finally, Section VIII concludes the paper.

II. Related Work

There exist some works focusing on delay analysis and optimization in CRNs [14]–[16], [23], [27]. Wang *et al.* [14] study SUs' queueing delay performance by taking a fluid queue approximation approach in which queue dynamics is

[1]The part of the work studied in this paper is submitted to IEEE Globecom 2018 and is accepted.

TABLE I
MAIN NOTATIONS AND DEFINITIONS

Notation	Definition	Notation	Definition
P_{tra}	Probability of SU(s) transmitting in a time slot	T_{slot}	Total duration of SUs' time slot
τ	SUs' conditional transmission probability	$\overline{T_{AD}}$	Access delay
T_{ss}	Time duration of spectrum sensing	M	Number of channels in CRNs
T_{tr}	Time duration of transmission period	N	Number of SUs in CRNs
T_{rt}	Time duration of Reserve Time in CHCS	ε	The detection threshold
T_{tx}	Time duration of a transmission in CHCS	W	Minimum contention window
P_b	Probability that channel is busy for SUs	m	Maximum backoff stage
P_i	Probability that channel is idle for SUs	p	Probability of a failed transmission
f_s	The sampling frequency of SUs in spectrum sensing	P_d	Probability of detection
γ	PUs' signal-to-noise ratio (SNR) received by SUs	P_f	Probability of false detection
P_I	Probability of interference probability to PUs	P_m	Probability of miss detection
P_{ERI}	Probability of SUs exchanging rendezvous information	P_{CSI}	Probability of sensing channel as idle
$P(n_s)$	Probability of n_s SUs achieving rendezvous on a channel	P_{BL}	Probability of establishing a link

represented as Poisson driven stochastic differential equations. Liang *et. al* [15] derive the average packet transmission delay for periodic switching channel scheme and triggered switching channel scheme, besides, for each switching scheme, they consider two types of real-time traffic, i.e., random burst of packets and Poisson arrival of packets. Even though these two works both consider multi-user contention in analyzing delay, they all assume that the spectrum sensing is perfect. Li *et al.* [16] analyze the expected per-hop delay incorporating the sensing delay and transmission delay in multi-hop multi-flow CRNs, considering imperfect spectrum sensing and transmission contention, but the analysis lacks of consideration of spectrum access mechanism (e.g., CCC or CH). Moreover, there is a type of delay resulted from the specific characteristics of designing an opportunistic spectrum access scheme in CRNs, e.g., [23], [27]. Hossain and Sarkar [23] propose a MAC scheme for CH based rendezvous with analysis of medium access delay and queueing delay; though it is claimed that quorum CH algorithm is used to establish the rendezvous, the impact of neither CH algorithm nor imperfect spectrum sensing on delay is considered. Liu *et al.* [27] analyze the impacts of rendezvous failure and neighbor contention on optimizing time slot and propose a simple MAC scheme for slot-asynchronous CH based rendezvous. However, the analysis is mainly based on the assumption of one neighbor SU, and the analysis also lacks of consideration of imperfect spectrum sensing and specific CH algorithm.

On the other hand, the increasing number of applications motivates the research on rendezvous-guaranteed CH sequence design (e.g., [1], [5]–[10], [19], [20], [26]). These works can be mainly divided into two categories: A) the design is based on the system or theory with inherent attribute like rotation closure property (RCP) which can achieve guaranteed rendezvous with different delay offsets [e.g., disjoint difference set [5], quorum system [7], [19], balanced incomplete block design (BIBD) [10], [20]], and B) the design is based on partially-random scheme with set pattern like jump-stay (hop-wait) mainly employing Mod operation, e.g., [1], [6], [8] and [9]. However, all above works fail to consider the impact of multi-SU transmission (e.g., collision). Therefore, Liu and Xie [21] analyze impact of collision and congestion on performance of rendezvous. They further develop a framework which can optimize system parameters to adapt to the dynamic network. However, they do not take into consideration the impacts, in practice, of detailed CH sequence and rendezvous scenarios.

Though the related works mentioned above focus on different aspects of CRNs, they fail to jointly take into consideration the impact of detailed operations in PHY layer (i.e., imperfect spectrum sensing) and MAC layer (i.e., exchanging information/data with specific CH or CCC scheme). Considering detailed operations surely helps performance evaluation more accurate.

III. SYSTEM MODEL AND PRELIMINARIES

For better readability, Table I shows the key notations used in describing our proposal. In this paper, we use different superscripts (i.e., ncs for CHNCS and cs for CHCS) to identify different functions and expressions which represent the same meaning.

We consider a distributed CRN where there are N SUs coexisting with PUs in the same geographical area. All SUs and PUs share the same set of non-overlapping M channels, and they all communicate with each other using a time-slotted method. Each SU is equipped with a half-duplex radio which is capable of detecting channel availability and switching among these M channels. Given that the channel switch overhead is in the order of microseconds [24] and the duration of a time slot is in the order of milliseconds (e.g., 10 ms in IEEE 802.22 [11]), we consider that the channel switch overhead is negligible.

SUs in distributed CRN are assumed to rendezvous with each other and further establish communication links. As shown in Fig. 3, a sender SU first senses the channel that it hops on. If the channel is sensed as idle, then the sender SU sends the rendezvous request (e.g., RTS) to try to establish a communication link with its receiver SU. If the sender SU receives the rendezvous acknowledgement (e.g., CTS) from its receiver SU successfully, this pair of SUs setup the link. However, if the channel is sensed as busy or the sender SU fails to receive the rendezvous acknowledgement in current time slot, it then hops on another channel in the next time slot and continues the sensing-access process. Hence, each time slot for both CHNCS and CHCS is composed of two parts:

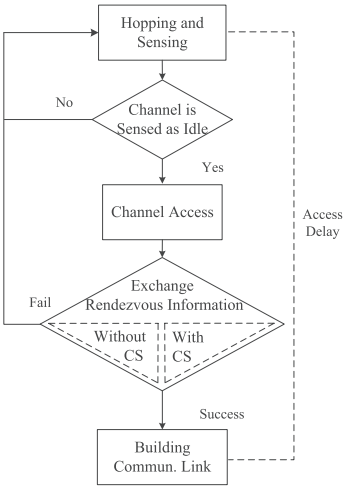

Fig. 3. Sensing-access process to establish communication link with CH scheme in multi-SU CRN.

spectrum sensing duration T_{ss} and transmission duration T_{tr} (shown in Figs. 1 and 2), i.e.,

$$T_{slot} = T_{ss} + T_{tr}. \tag{1}$$

In CRNs, channel state is determined by PUs' activities. The PU's traffic is modeled as a 1-0 renewal process [12] where "1" represents that the channel is busy in a time slot and "0" represents the channel is idle. To simplify the analysis, we assume that the channel state is steady during the time slot and the average time holding for state "1" is α and β for state "0". Therefore, in any time slot, the channel is busy with probability $P_b = \frac{\alpha}{\alpha+\beta}$ and idle with probability $P_i = \frac{\beta}{\alpha+\beta}$.

It is worth noting that the objective is to minimize access delay by optimizing both PHY and MAC parameters in CH-based multi-channel multi-SU distributed CRNs. Indeed, we do not consider data throughput (i.e., data transmission in a time slot) in the proposed access delay model. Hence, we assume that SUs, during T_{tr}, attempt to exchange only rendezvous information. Data transmission operations can be performed by SUs with some specific protocols ([3], [11]). This assumption minimizes the impact of data transmission scheme on establishing communication links. Thus, we can establish a general purpose access delay model, which can be easily adapted to different protocols with specific transmission schemes.

A. Spectrum Sensing

To make the proposed optimization approach generally applicable, we adopt the widely used energy detection scheme [11], [12], [22] to perform spectrum sensing. Therefore, according to [12], the probability of false detection is then given by

$$P_f(\varepsilon, T_{ss}) = \Pr(Y > \varepsilon | H_0) = \frac{1}{2}\mathrm{erfc}\left(\frac{\varepsilon - f_s T_{ss}}{2\sqrt{f_s T_{ss}}}\right), \tag{2}$$

where Y is the sensing result which is the sum of samples, ϵ denote the detection threshold, f_s represent the sampling frequency, H_0 denotes the hypothesis that the licensed channel is unoccupied and $\mathrm{erfc}(\cdot)$ is the complementary error function of the standard Gaussian [22]. Under hypothesis H_1 that the PU is active on the licensed channel, let $\gamma = \sigma_s/\sigma_n$ denote the PUs' signal-to-noise ratio (SNR) measured at the SUs' receiver; the probability of detection can be derived as

$$P_d(\varepsilon, T_{ss}) = \Pr(Y > \varepsilon | H_1) = \frac{1}{2}\mathrm{erfc}\left(\frac{\varepsilon - f_s T_{ss}(1+\gamma)}{2\sqrt{f_s T_{ss}(1+2\gamma)}}\right), \tag{3}$$

and the probability of miss detection can be expressed as

$$P_m(\varepsilon, T_{ss}) = \Pr(Y < \varepsilon | H_1) = 1 - P_d(\varepsilon, T_{ss}). \tag{4}$$

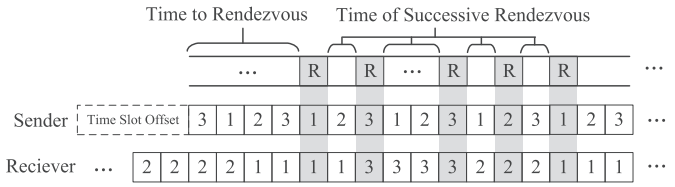

Fig. 4. Illustration of TTR and TSR. The "R" in gray blocks means the rendezvous time slots and numbers represent channel indices.

B. Access Delay

If the sender SU wants to establish a communication link with its receiver SU, they should first achieve rendezvous by following CH sequences. The process is depicted in Fig. 4, where SUs spend *Time To Rendezvous* (*TTR*) to achieve first rendezvous, or they have to spend *Time of Successive Rendezvous* (*TSR*) for each rendezvous after they fail to achieve the first rendezvous. The success or failure of each rendezvous relates to two conditions: 1) Access the channel as SUs sense the channel is idle (with probability P_{CSI}), and 2) SUs exchange RTS/CTS successfully on the rendezvous channel (with probability P_{ERI}).

P_{CSI} relates to PUs' activity and SUs' sensing results. If Y is smaller than ϵ, the channel is idle; this can be represented as $P_{CSI} = \mathrm{P_r}(Y < \varepsilon)$. Considering miss detection, false detection and PUs' activities, the probability of channel being sensed idle is expressed as

$$\begin{aligned} P_{CSI} &= \Pr(Y < \varepsilon | H_0)\Pr(H_0) + \Pr(Y < \varepsilon | H_1)\Pr(H_1) \\ &= (1 - P_f(\varepsilon, T_{ss})) \cdot P_i + P_m \cdot P_b. \end{aligned} \tag{5}$$

Let "A" denote the event that the channel sensed by a SU is idle and "E" denote the event that the SU succeeds in transmission contention. The probability P_{BL} that the SU establishes a communication link with its receiver can be expressed as

$$\begin{aligned} P_{BL} &= \Pr(\mathrm{AE}) = \Pr(\mathrm{A})\Pr(\mathrm{E}|\mathrm{A}) \\ &= P_{CSI}(\varepsilon, T_{ss}, T_{tr}) \cdot P_{ERI}(\varepsilon, T_{ss}, T_{tr}), \end{aligned} \tag{6}$$

where $P_{ERI}(\varepsilon, T_{ss}, T_{tr})$ represents $\Pr(\mathrm{E}|\mathrm{A})$.

Furthermore, let *ATTR* represent the average number of time slots that SUs take for achieving the first rendezvous, and let *ATSR* denote average number of time slots taken for successive

rendezvous, then expected access delay $\overline{T_{AD}}$ for CHNCS can be expressed as

$$\begin{aligned}\overline{T_{AD}^{ncs}} &= T_{slot}\cdot[(ATTR+1)P_{BL} \\ &\quad + \sum_{n=1}^{\infty} P_{BL}(1-P_{BL})^n(ATTR+1+n(ATSR+1))] \\ &= T_{slot}^{ncs}\cdot[ATTR+1+\frac{1-P_{BL}^{ncs}}{P_{BL}^{ncs}}\cdot(ATSR+1)].\end{aligned} \tag{7}$$

where T_{slot} represents the duration of the time slot. Similarly, for CHCS, the access delay is

$$\overline{T_{AD}^{cs}} = T_{slot}^{cs}\cdot[ATTR+1+\frac{1-P_{BL}^{cs}}{P_{BL}^{cs}}\cdot(ATSR+1)]+\overline{\Delta}, \tag{8}$$

where $\overline{\Delta}$ is average time duration consumed for contention in the rendezvous time slot.

Both Eq. 13 and Eq. 14 indicate that SUs on average undergoes $\frac{1-P_{BL}^{cs}}{P_{BL}^{cs}}$ rendezvous failures including failure in first attempt of rendezvous. The difference of access delay between CHCS and CHNCS lies on whether CS is employed or not, i.e., T_{slot}, $P_{ERI}(\varepsilon, T_{ss}, T_{tr})$ and $\overline{\Delta}$.

IV. Analysis of Transmission in a Time Slot

In distributed CRNs, SUs are likely to randomly select CH sequences generated by CH algorithm. Some existing CH algorithms [5], [7], [9], [10], [19], [20] are able to regulate SUs to hop uniformly between channels. Hence, we assume that each SU hops on and senses a specific channel with probability $1/M$. Then, the probability that the other n_s SUs hop on and sense the same channel with the corresponding SU can be expressed as

$$P(n_s)=C_{N-1}^{n_s}\cdot\left(\frac{1}{M}\right)^{n_s}\cdot\left(\frac{M-1}{M}\right)^{N-1-n_s}, \quad n_s\le N-1. \tag{9}$$

Once multiple SUs hop on the same channel and sense it as idle, they will transmit RTS/CTS immediately in the case of CHNCS or contend for the channel in the case of CHCS. In both scenarios, the SUs suffer from two kinds of failed transmissions: (a) collisions with SU's and/or PUs' transmissions and (b) SUs fail to achieve rendezvous.

Let P_c denote the probability of transmission collision, P_c can be expresses as

$$P_c = P_c^s + P_c^p - P_c^s\cdot P_c^p, \tag{10}$$

where P_c^s (P_c^p) is the probability that the transmission collides with other SUs' (PUs') transmissions. Collisions with other SUs occur only when at least one of the n_s SUs transmit. Let τ denote the transmission probability; P_c^s can be expressed as

$$P_c^s = \sum_{n_s=1}^{N-1} P(n_s)\cdot(1-(1-\tau)^{n_s}). \tag{11}$$

The transmission collides with PUs' transmissions only when miss detection occurs. Then, P_c^p can be expresses as

$$P_c^p = P_m(\varepsilon, T_{ss})\cdot P_b. \tag{12}$$

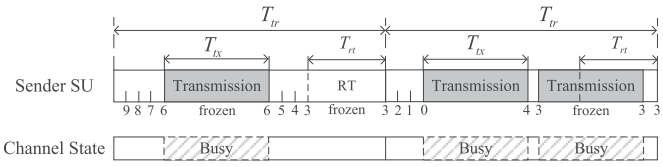

Fig. 5. Transmission scheme of IEEE 802.11 DCF adopted in CH-based CRNs.

A. Multi-SU Transmission for CHNCS

In the CHNCS scenario, SUs only need to transmit RTS/CTS for one time during the entire duration of the time slot. Hence, T_{tr} is fixed and can be expressed as

$$T_{tr}^{ncs} = t_{RTS} + t_{CTS} + \text{SIFS}, \tag{13}$$

where t_{RTS} and t_{CTS} denote the transmission duration of RTS and CTS respectively; SIFS is short for 'short interframe space' defined in IEEE 802.11 standard.

Due to the fact that SUs in CHNCS will transmit immediately once they sense the channel idle, τ for CHNCS in Eq. (11) can be expressed as

$$\tau^{ncs} = 1. \tag{14}$$

Then, $P_{ERI}(\varepsilon, T_{ss}, T_{tr})$ for CHNCS can be expressed as

$$P_{ERI}^{ncs}(\varepsilon, T_{ss}, T_{tr}) = 1 - P_c(\tau^{ncs}). \tag{15}$$

B. Multi-SU Transmission for CHCS

In the CHCS scenario, SUs employ CS to transmit RTS/CTS on the same channel distributedly. Since IEEE 802.11 DCF-based CSMA/CA has been widely used in distributed wireless networks, we adopt the CS which is similar to IEEE 802.11 DCF to regulate the transmissions in CHCS. As the same in IEEE 802.11 DCF, when the backoff counter decreases to zero, the SU starts to transmit; otherwise, it continues to decrease its backoff counter or freezes the counter when it detects other SUs transmitting.[2] The difference is that, in conventional wireless networks, users do not need to hop between channels during the contention-transmission process, while, with slot-by-slot structure in multi-channel CRNs, SUs have to hop on different channels after a fixed period (i.e., T_{slot}). It may happen that after an SU wins a transmission opportunity by CS, the time left in this time slot is not enough for the transmission. To avoid this, a Reserve Time (RT) (denoted by T_{rt}) which has a minimal duration required for exchanging RTS/CTS is placed in the end of each time slot (see Fig. 5, for better clarity, the sensing operation is ignored). Then, the durations of a transmission and RT are expressed as

$$T_{tx} = t_{RTS} + t_{CTS} + \text{SIFS} + \text{DIFS} \tag{16a}$$

$$T_{rt} = t_{RTS} + t_{CTS} + \text{SIFS}. \tag{16b}$$

[2]To avoid the channel busy time-inconsistency problem [17], each SU freezes its backoff counter for a duration of T_{tx} when it detects a transmission that is no matter successful or not.

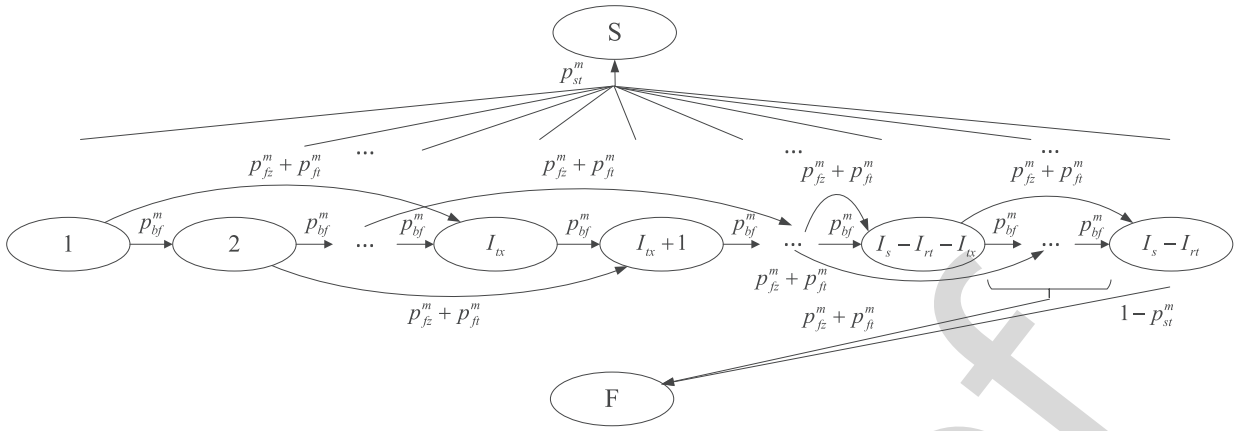

Fig. 6. State transition process of the corresponding SU in one time slot.

To derive $P_{ERI}^{cs}(\varepsilon, T_{ss}, T_{tr})$, we model the contention-transmission process as an absorbing Markov chain. The duration of T_{tr}^{cs} is subdivided into I_s backoff slots to construct a discrete time system; all backoff slots in each T_{tr}^{cs} are labeled as $1, \ldots, I_s$. Correspondingly, the durations of T_{rt}^{cs} and T_{tx}^{cs} are subdivided into I_{rt} and I_{tx} bakcoff slots, respectively. Note that if SUs fail to seize the opportunity within the first $(I_s - I_{rt})$ backoff slots, they will fail to establish communication links in current time slot. Hence, we only consider these $(I_s - I_{rt})$ backoff slots.

During transmission contention process, as shown in Fig. 6, SUs may encounter one of the four possible events: 1) backoff operation, with probability p_{bf}; 2) backoff counter frozen due to other SUs' transmissions, with probability p_{fz}; 3) a failed transmission of the corresponding SU, with probability p_{ft}; and 4) a successful transmission of the SU, with probability p_{st}. The probabilities of the four events can be expressed as

$$p_{bf} = (1-\tau) \cdot \sum_{n_s=0}^{N-1} P(n_s) \cdot (1-\tau)^{n_s} \tag{17a}$$

$$p_{st} = \tau \cdot \sum_{n_s=0}^{N-1} P(n_s) \cdot (1-\tau)^{n_s} \tag{17b}$$

$$p_{fz} = (1-\tau) \cdot \sum_{n_s=1}^{N-1} P(n_s) \cdot (1-(1-\tau)^{n_s}) \tag{17c}$$

$$p_{ft} = \tau \cdot \sum_{n_s=1}^{N-1} P(n_s) \cdot (1-(1-\tau)^{n_s}). \tag{17d}$$

According to Bianchi's research [29], τ in Eqs. (11) and (17) can be derived as

$$\tau^{cs} = \frac{2\,(1-2p^{cs})}{(1-2p^{cs})\,(W+1) + p^{cs} W\,(1-(2p^{cs})^m)}, \tag{18}$$

where W denotes the minimum contention window, m denotes the maximum backoff stage and p^{cs} is the probability of a failed transmission. Considering failed transmissions due to failed rendezvous, p^{cs} can be expressed as

$$p^{cs} = 1 - (1-P_c) \cdot P_{ren}, \tag{19}$$

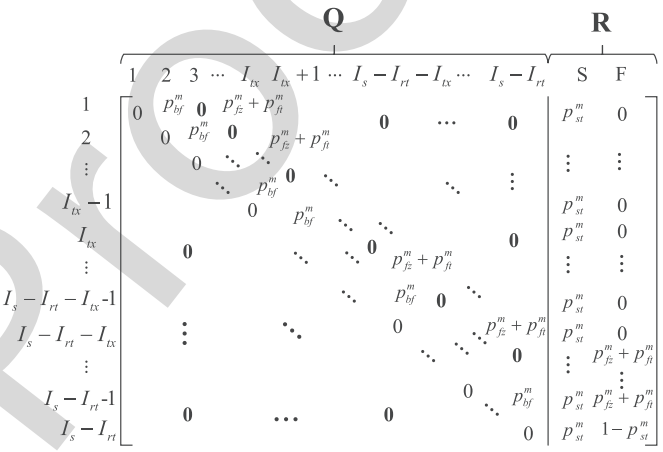

Fig. 7. One-step transition probability matrix of the absorbing Markov chain.

where P_{ren} represents the probability that SUs achieve rendezvous (details are in Section V).

In Fig. 6, SUs finally falls into one of the two absorbing states: 1) "S": successfully establishing a communication link in current time slot and 2) "F": failing to establish a communication link. We can formulate the canonical form of one-step transition probability matrix P as

$$\mathrm{P} = \begin{bmatrix} \mathrm{Q} & \mathrm{R} \\ 0 & \mathrm{I} \end{bmatrix}, \tag{20}$$

where I is the identity matrix and R is the probability matrix of sates "S" and "F" (see Fig. 7).

According to the Markov chain theory [30], the n-step transition probability matrix without absorbing states can be expressed as Q^n in which the element $(\mathrm{Q}^n)_{i,j}$ is the (ij)th entry of the matrix. $(\mathrm{Q}^n)_{ij}$ is also the probability that a SU transits from $state\ i$ to $state\ j$ with n steps. Thus, the probability p_{ij}^I that an SU transits from $state\ I_i$ to $state\ I_j$ can be expressed as

$$p_{ij}^I = \sum_{k=0}^{\infty} \left(\mathrm{Q}^k\right)_{ij}. \tag{21}$$

Let P^I denote the transition probability matrix which is composed of elements p_{ij}^I $(1 \le i,j \le I_s - I_{rt})$.

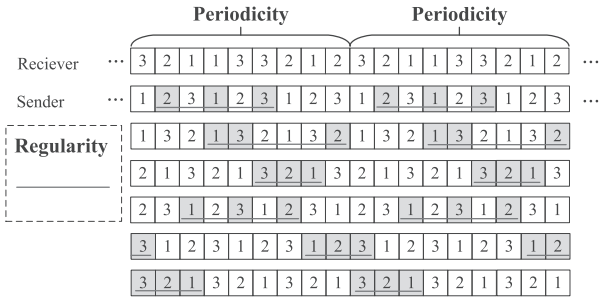

(a) The periodicity and the regularity of ACH

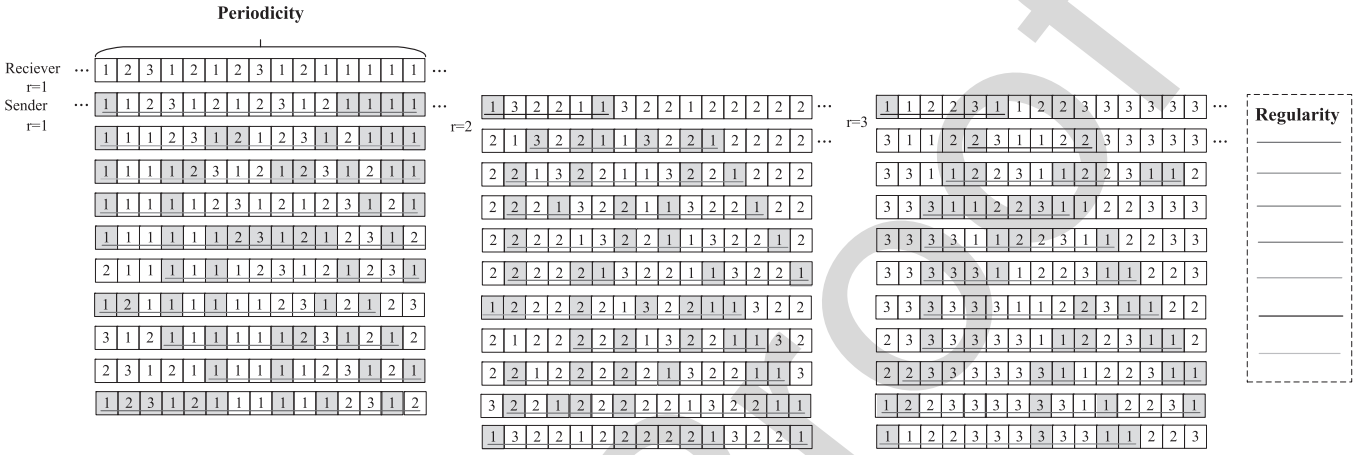

(b) The periodicity and the regularity of JS, r represents step length chosen from (1,M) where M is number of channel

Fig. 8. Examples of rendezvous algorithms.

Since submatrix Q is a strict upper triangular matrix, P^I can be expressed as

$$\mathrm{P}^I = \sum_{k=0}^{\infty} \mathrm{Q}^k = \sum_{k=0}^{I_s - I_{rt}} \mathrm{Q}^k = (\mathrm{I} - \mathrm{Q})^{-1}. \tag{22}$$

In each time slot, an SU always starts from the beginning of the time slot (i.e., the state I_1). Hence, P_{ERI} for CHCS can be expressed as

$$P_{ERI}^{cs}(\varepsilon, T_{ss}, T_{tr}^{cs}) = \left(\mathrm{P}^I \mathrm{R}\right)_{11} = \sum_{j=1}^{I_s - I_{rt}} \left(\mathrm{P}^I\right)_{1j} \cdot p_{st}. \tag{23}$$

Then, $\overline{\Delta}$ can be expressed as

$$\overline{\Delta} = \sum_{j=1}^{I_s - I_{rt}} j \cdot \left(\mathrm{P}^I\right)_{1j} \cdot p_{st}. \tag{24}$$

V. Analysis of CH-Based Rendezvous

A key condition for SUs to establish a link is to achieve rendezvous. For the sake of analysis, we assume that the PU activity is unchanged during the rendezvous process. Due to the fact that SUs can start a CH rendezvous process in a random time slot, the probabilities that SUs start hopping in time slot i or time slot j are equal. Then, the relationship between $ATTR$ and $ATSR$ is expressed as

$$ATTR = \frac{ATSR + 1}{2}. \tag{25}$$

The A-type CH algorithms (see Section II) have inherent regularity in CH sequences and thus it is easy to derive $ATSR$ of these algorithms. The B-type CH algorithms (see Section II) usually use prime number modular arithmetic to guarantee rendezvous, which can be seen as a circle walk on a clock. However, the ***regularity*** and the ***periodicity*** of these CH algorithms can still be derived via the analysis. The ***regularity*** means that there are several rendezvous patterns in a rendezvous algorithm, and all rendezvous scenarios are contained in these rendezvous patterns. In each pattern, rendezvous always occurs periodically, which is the ***periodicity***. We can employ the ***regularity*** to determine average number of rendezvous slots in a ***periodicity***. To be more specific, different rendezvous patterns of the CH algorithm contain different numbers of rendezvous slots (see Fig. 8). Then, the average number of rendezvous slots in a ***periodicity*** with M channels can be expressed as

$$E\left[R_M\right] = \sum^{\Omega} n_{ren}^i \cdot p_{ren}^i \quad (\forall i,\ i \in \Omega), \tag{26}$$

where n_{ren}^i and p_{ren}^i represent the number of rendezvous slots in $pattern\ i$ and the corresponding proportion respectively, and Ω is set of all rendezvous patterns.

Fig. 8 shows examples of the ***regularity*** and the ***periodicity*** of two typical CH algorithms (i.e., ACH [7] and JS [8]), where there are 3 channels and time slots with the same underline color belonging to same ***regularity***. Because of the limited space, we do not present detailed analysis of these algorithms.

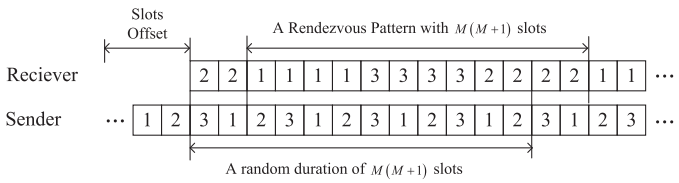

Fig. 9. Illustration of the rendezvous pattern.

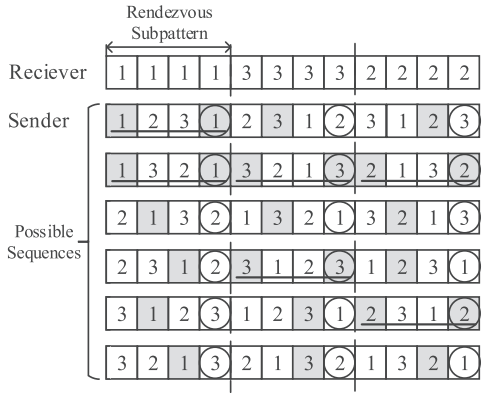

Fig. 10. Examples of rendezvous patterns.

In this paper we take recent Sender Jump-Receiver Wait (SJ-RW) [9] as an example to analyze the $ATSR$ due to its outstanding performance, which can represent the recent advance in this area. In SJ-RW algorithm, the period of the rendezvous pattern is $M(M+1)$ time slots. Every overlap of $M(M+1)$ time slots between any pairwise sequences (i.e., a sender's and a receiver's sequences) is equal to a rendezvous pattern with $M(M+1)$ time slots (see Fig. 9 and refer to [9] for more details).

In SJ-RW, the sender stays on a channel for a time slot while the receiver for $M+1$ time slots. Hence, the sender repeats visiting one channel after visiting all channels when the receiver waits on the channel for $M+1$ time slots, which represents a rendezvous subpattern. More specifically, this indicates that if the repeating channel is the same channel that the receiver waits on, then during these $M+1$ time slots there exist two rendezvous slots; we call this rendezvous subpattern as *Two-Rendezvous Subpattern* (see underlined successive time slots in Fig. 10), and the others *One-Rendezvous Subpattern*. Furthermore, if channel-visiting order of sender is the same with that of the receiver, then there will be M Two-Rendezvous Subpatterns and in total $2M$ rendezvous slots in a rendezvous pattern (see the second sequence in Fig. 10, i.e., there are 3 Two-Rendezvous Subpatterns in this rendezvous pattern).

We can determine that for a specific channel, if the sender's channel-visit order of this channel is the same as the receiver's, the Two-Rendezvous Subpattern occurs; otherwise, the One-Rendezvous Subpattern occurs. Furthermore, we can conclude that permutations and combinations of Two-Rendezvous Subpatterns and One-Rendezvous Subpatterns are equivalent to the differences between sender's and receiver's channel-visit orders. This can be modeled as the Derangement Problem in Discrete Mathematics [28]. We refer to the same channel that the sender and receiver visit in a different order as the *derangement channel*. According to the principle of inclusion-exclusion, the number of patterns with k derangement channels $D(k)$ can be expressed as

$$D(k) = k!\left(\sum_{r=2}^{k}(-1)^r\frac{1}{r!}\right) \quad (k \geq 2). \tag{27}$$

$E[R_M]$ can be derived as

$$E[R_M] = \sum_{d=2}^{M}(2M-d)\cdot\frac{\mathrm{C}_M^d \cdot D(d)}{M!} + \frac{2}{(M-1)!}, \tag{28}$$

where d is the number of the derangement channels. Then, $ATSR$ can be expressed as

$$ATSR = \frac{M(M+1) - E[R_M]}{E[R_M]}. \tag{29}$$

From a long run of CH process, P_{ren} can be derived as

$$P_{ren} = \frac{1}{ATSR+1}. \tag{30}$$

Thus, we now get closed-form expressions of $ATTR$ and $ATSR$ to further formulate access delay for CHCS and CHNCS.

VI. Optimization Models and Algorithms

The objective is to minimize access delays of both CHNCS and CHCS by jointly optimizing ε and T_{ss}, using the proposed access delay model. In order to easily obtain optimized parameters in online applications, a Bio-inspired Fast Search (BFS) algorithm for CHNCS and a Step-length Adaptation based Fast Search (SAFS) algorithm for CHCS are proposed to search for the optimal parameters and calculate the corresponding minimum access delay, respectively.

A. Interference Probability Constraint

In order to ensure that PUs have the highest priority to access spectrum, an interference probability threshold is set to protect PUs from SUs' interference in both CHNCS and CHCS scenarios.

Actually, it is possible for SUs' transmissions colliding with PUs' if miss detections occur and at least one SU transmits during T_{tr}. Then, the interference probability can be expressed as

$$P_I(\varepsilon, T_{ss}) = P_b \cdot P_m(\varepsilon, T_{ss}) \cdot P_{tra} \tag{31}$$

where P_{tra} is the conditional probability that at least one SU transmits during T_{tr}, given that the channel is sensed idle.

B. Optimization for CHNCS

For CHNCS, due to Eq. (14), P_{tra} in Eq. (31) can be expressed as

$$P_{tra}^{ncs} = 1. \tag{32}$$

Then, $P_I(\varepsilon, T_{ss})$ can be expressed as

$$P_I^{ncs}(\varepsilon, T_{ss}) = P_b \cdot P_m(\varepsilon, T_{ss}). \tag{33}$$

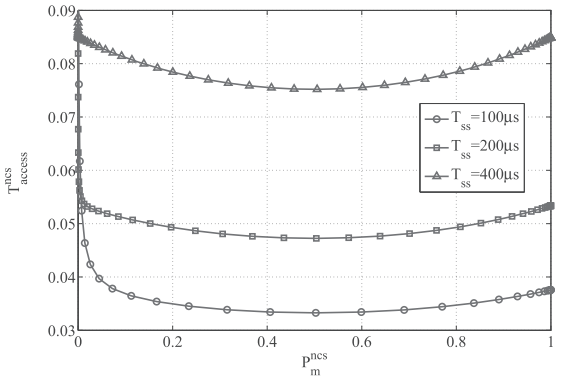

Fig. 11. P_m^{ncs} vs. T_{access}^{ncs} in varied T_{ss}.

The optimization model on the access delay can be formulated as

$$\underset{\varepsilon, T_{ss},}{\text{minimize}} \ \overline{T_{AD}^{ncs}}$$
$$\text{subject to } P_I^{ncs}(\varepsilon, T_{ss}) \le \bar{P}_I, \tag{34}$$

We run extensive simulations (i.e., exhaustive search on T_{ss}^{ncs}) to minimize T_{access}^{ncs}; we found that the relation between P_m^{ncs} and T_{access}^{ncs} may not be monotone. For example, Fig. 11 shows that T_{access}^{ncs} first deceases and increases with increasing P_m^{ncs}. That is to say, for a given T_{ss}^{ncs} and $\bar{P}_I$, the optimal ε_{opt}^{ncs} may satisfy $P_I^{ncs}(\varepsilon_{opt}^{ncs}, T_{ss}^{ncs}) < \bar{P}_I$. Then, we use Firefly Algorithm [13] to develop a Bio-inspired Fast Search (BFS) algorithm to search for the optimal ε and T_{ss}. **Algorithm 1** shows the pseudo-code of the algorithm.

In **Algorithm 1**, F_{access}^{ncs} is the formulation of access delay which can be obtained using Eqs. (5)–(7), (13) and (15). $\mathrm{Rand}(1)$ is the function that generates float number within (0,1). Light is the array of light intensity value of all fireflies, in ascending order. Lines 6-10 indicate that firefly i with smaller light intensity moves towards firefly j with larger light intensity and the step length is restrained by α, β and θ, which represent randomness factor, directional strength and absorption coefficient respectively. Lines 11-14 make sure that each firefly moves within the search range. Line 16 accelerates convergence of the firefly algorithm.

C. Optimization for CHCS

For CHCS, during T_{tr}^{cs} there exist I_s backoff slots; let $\hat{P}_{tra}$ represent the probability that at least one SU transmits in a backoff slot. P_{tra} can be expressed as

$$P_{tra}^{cs} = 1 - \left(1 - \hat{P}_{tra}\right)^{I_s}, \tag{35}$$

where $\hat{P}_{tra}$ can be expressed as

$$\hat{P}_{tra} = 1 - (1 - \tau^{cs}) \cdot \sum_{n_s=0}^{N-1} P(n_s) \cdot (1 - \tau^{cs})^{n_s}. \tag{36}$$

Then, $P_I(\varepsilon, T_{ss})$ can be expressed as

$$P_I^{cs}(\varepsilon, T_{ss}) = P_b \cdot P_m(\varepsilon, T_{ss}) \cdot P_{tra}^{cs}. \tag{37}$$

Algorithm 1 : BFS Algorithm for CHNCS

1: **Input**: number of fireflies N_F, maximum number of iterations I^{Max}, search range of T_{ss} (from T_{ss}^{min} to T_{ss}^{max}).
2: Scaling of search range: $S_R = |T_{ss}^{min} - T_{ss}^{max}|$
3: Initialize positions of N_F fireflies: $T_{ss}^i = \mathrm{Rand}(1) \cdot S_R$ and $\varepsilon^i = \mathrm{Rand}(1) \cdot \bar{\varepsilon}(T_{ss}^i)$[3]
4: **for** $I = 1 : MaxI$ **do**
5: Update Light Intensity $Light^i$ of each firefly: $Light^i = 1/F_{access}^{ncs}(\varepsilon^i, T_{ss}^i)$
6: **if** $Light^i < Light^j$ **then**
7: $r = \sqrt{\left(T_{ss}^i - T_{ss}^j\right)^2 + \left(\varepsilon^i - \varepsilon^j\right)^2}$.
8: $\beta = (1 - \beta_{\min}) \cdot \exp(-\theta r^2) + \beta_{\min}$.
9: $T_{ss}^i = T_{ss}^i(1-\beta) + T_{ss}^j\beta + \alpha(\mathrm{Rand}(1) - 0.5) \cdot S_R$.
10: $\varepsilon^i = \varepsilon^i(1-\beta) + \varepsilon^j\beta + \alpha(\mathrm{Rand}(1) - 0.5) \cdot \bar{\varepsilon}(T_{ss}^i)$.
11: **if** $T_{ss}^i \le T_{ss}^{min}$ **then** $T_{ss}^i = T_{ss}^{min}$ **end if**
12: **if** $T_{ss}^i \ge T_{ss}^{max}$ **then** $T_{ss}^i = T_{ss}^{max}$ **end if**
13: **if** $\varepsilon^i \le 0$ **then** $\varepsilon^i = 0$ **end if**
14: **if** $T_{ss}^i \ge \bar{\varepsilon}(T_{ss}^i)$ **then** $\varepsilon^i = \bar{\varepsilon}(T_{ss}^i)$ **end if**
15: **end if**
16: $\alpha = (\frac{10^{-3}}{9})^{\frac{1}{MaxI}} \cdot \alpha$ //reduce randomness
17: $[\mathrm{Light}, \mathrm{Index}] = \mathrm{Sort}([\mathrm{Light}^1, \ldots, \mathrm{Light}^{\mathrm{N_F}})$
18: **end for**
19: $T_{ss} = T_{ss}(Index)$ and $\varepsilon = \varepsilon(Index)$
20: $T_{ss}^{opt} = T_{ss}^{N_F}$, $\varepsilon^{opt} = \varepsilon^{N_F}$ and $T_{access}^{min} = 1/Light^{N_F}$
21: **Output**: the optimal T_{ss} is T_{ss}^{opt}, the optimal ε is ε^{opt} and the minimum T_{access} is T_{access}^{min}.

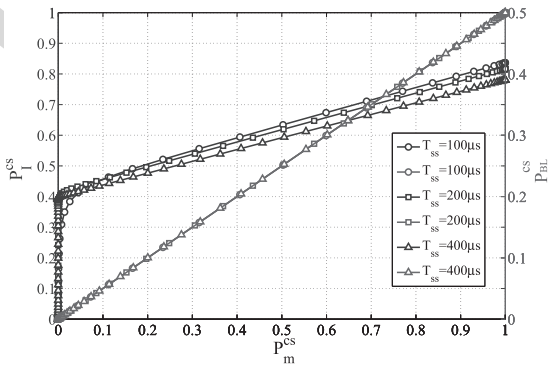

Fig. 12. P_m^{cs} vs. P_I^{cs} in varied T_{ss}.

The optimization model on access delay can be formulated as

$$\underset{\varepsilon, T_{ss},}{\text{minimize}} \ \overline{T_{AC}^{cs}}$$
$$\text{subject to } P_I^{cs}(\varepsilon, T_{ss}) \le \bar{P}_I. \tag{38}$$

According to Eqs. (4) and (35)–(37), P_I^{cs} is an increasing function of P_m^{cs} (see Fig. 12). P_{BL}^{cs} is also monotonically increasing with respect to P_m^{cs} (see Fig. 12). Besides, larger ε results in larger P_m^{cs} due to the fact that P_m^{cs} is an increasing

[3] $\bar{\varepsilon}(T_{ss})$ is the function of upper limit of ε that satisfy $P_I^{ncs}(\varepsilon, T_{ss}) \le \bar{P}_I$ for given T_{ss}, which is $\mathrm{erfcinv}(1 - \frac{\bar{P}_I}{P_b}) \cdot 2\sqrt{f_s T_{ss}(1+2\gamma)} + f_s T_{ss}(1+\gamma)$ where $\mathrm{erfcinv}(\cdot)$ is the inverse function of complementary error function.

Algorithm 2 : SAFS Algorithm for CHCS

1: **Input**: regular search step length S_{reg}, minimum search step length S_{min}, initial searching point T_{ss}^{ini}, end search point T_{ss}^{end}.
2: Initialize access delay T_{access}^{0} for the given T_{ss}^{ini} according to $F_{access}^{cs}(T_{ss})$.
3: **while** $T_{ss}^{i} < T_{ss}^{end}$[4] **do**
4: $T_{ss}^{i} = T_{ss}^{i-1} + \Gamma(\lambda) S_{reg}$.[5]
5: Update T_{access}^{i} with T_{ss}^{i} according to $F_{access}^{cs}(T_{ss})$
6: $\lambda^{i} = (T_{access}^{i} - T_{access}^{i-1})/(T_{ss}^{i} - T_{ss}^{i-1})$
7: **if** $\lambda^{i} \cdot \lambda^{i-1} \leq 0$ **then**
8: **for** $T_{ss}^{j} = T_{ss}^{i-2} : S_{min} : T_{ss}^{i}$ **do**
9: Update T_{access}^{j} with T_{ss}^{j} according to $F_{access}^{cs}(T_{ss})$
10: **if** $T_{access}^{j} \leq T_{access}^{j-1}$ **then**
11: $T_{access}^{min} = T_{access}^{j}$, $T_{ss}^{opt} = T_{ss}^{j}$
12: **end if**
13: **end for**
14: **end if**
15: **end while**
16: **Output**: the optimal T_{ss} is T_{ss}^{opt} and the minimum T_{access} is T_{access}^{min}.

function of ε according to Eqs. (3) and (4). Hence, we have the following corollary:

Corollary 1: The optimal values of ε and T_{ss}, which satisfy $P_I^{cs}(\varepsilon, T_{ss}) \leq \bar{P}_I$ and minimize the access delay T_{access}^{cs} are given by $(\varepsilon^*, T_{ss}^*)$, where $P_I^{cs}(\varepsilon^*, T_{ss}^*) = \bar{P}_I$.

Proof: If we assume that the optimal values of ε and T_{ss} exist such that $P_I^{cs}(\varepsilon^*, T_{ss}^*) < \bar{P}_I$, and there exists a ε^0, such that $\varepsilon^0 > \varepsilon^*$, then, we will have $P_I^{cs}(\varepsilon^0, T_{ss}^*) > P_I^{cs}(\varepsilon^*, T_{ss}^*)$ and $P_m^{cs}(\varepsilon^0, T_{ss}^*) > P_m^{cs}(\varepsilon^*, T_{ss}^*)$ resulting in $P_{BL}^{cs}(\varepsilon^0, T_{ss}^*) > P_{BL}^{cs}(\varepsilon^*, T_{ss}^*)$. Hence, we can conclude that for any given T_{ss}, the optimal ε^{opt} must satisfy $P_I^{cs}(\varepsilon^{opt}, T_{ss}) = \bar{P}_I$ ■

Using Corollary 1, we can reduce the search space of (ε, T_{ss}), and thus the search complexity, by converting a two-dimension solution space to one-dimension solution space. Then, we develop a Step-length Adaptation based Fast Search (SAFS) algorithm, to search for the optimal parameter T_{ss}^{opt} and calculate the corresponding minimum T_{access}^{min}. **Algorithm 2** shows the pseudo-code of the algorithm.

In **Algorithm 2**, $F_{access}^{cs}(T_{ss})$ is the formulation of access delay function which can be obtained using Eqs. (5), (6), (8), (23) and (24). $\Gamma(\lambda)$ is a function for adjusting step length of the search and is equal to $\Gamma(\lambda) = \frac{\mathrm{e}}{1+\mathrm{e}^{-\lambda^2}} - 0.65$ where e is Euler Number; S_{reg} and S_{min} are $25\mu s$ and $2\mu s$, respectively. Line 4 indicates that λ is the slope of at least one point between two adjacent step points (e.g., T_{ss}^{i} and T_{ss}^{i-1}) on the curve of $F_{access}^{cs}(T_{ss})$ according to Lagrange Mean Value Theorem. Line 5 indicates that there is at least one minimum value of T_{access} in $[T_{ss}^{i-2}, T_{ss}^{i}]$ (i.e., where the adjacent slopes are neither positive nor negative). Then, in $[T_{ss}^{i-2}, T_{ss}^{i}]$, exhaustive search on parameter T_{ss}, is used to counteract the possibility of missing optimal value using the non-exhaustive search.

[4] $T_{ss}^{i=0}$ represents T_{ss}^{ini}.
[5] λ is initialized to 0.1 at the beginning.

TABLE II
SIMULATION PARAMETER AND VALUE

Parameter	Value	Parameter	Value
Channel bandwidth	4 MHz	PUs' SNR received by SUs	-7 db
Transmission rate	2 Mbps	Interference probability threshold	5 %
Data length of CTS	128 bit	SIFS for CHCS	10 μs
Data length of RTS	128 bit	DIFS for CHCS	50 μs
Backoff slot	20 μs	Duration of time slot for CHCS	2 ms

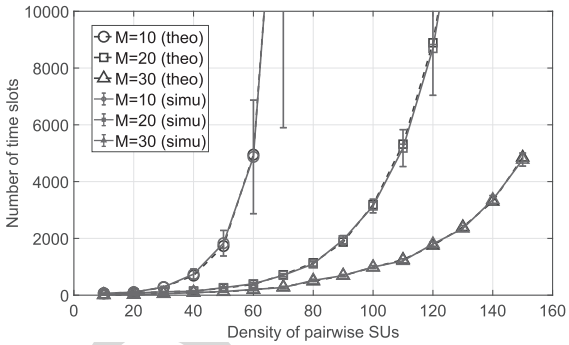

Fig. 13. Verification of access delay model for CHNCS with criteria of time slot.

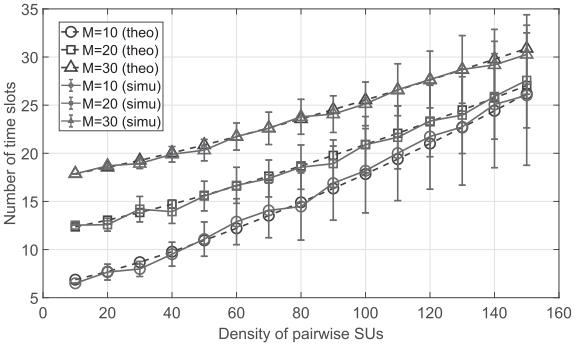

Fig. 14. Verification of access delay model for CHCS with criteria of time slot.

VII. SIMULATION AND ANALYSIS

In this section, the proposed model is validated and the impact of spectrum sensing and multi-SU contention on access delay is analyzed through extensive simulations. In simulations, all SUs are randomly deployed within a space of 100m $\times$ 100m, and each SU has a transmission range of 150m. The P_i and P_b are both 0.5. The experimental results are mean values from 150 independent simulations. Other simulation parameters are listed in Table II.

A. Validation of Theoretical Model

In this subsection, we validate the rendezvous formulation and multi-SU contention model in terms of time slots taken for successfully establishing communication links, for both CHNCS and CHCS without considering PUs' activities. In simulations, SUs can hop on and try to establish links on all channels (i.e., P_{CSI} is equal to 1 for every channel in the theoretical model). The results are shown in Fig. 13 for CHNCS and Fig. 14 for CHCS. The theoretical results perfectly match simulation results in Fig. 13 while

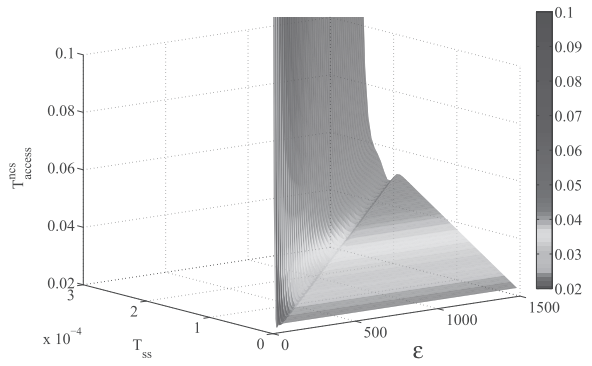

Fig. 15. Access delay jointly impacted by sensing duration and detection threshold in CHNCS scenario.

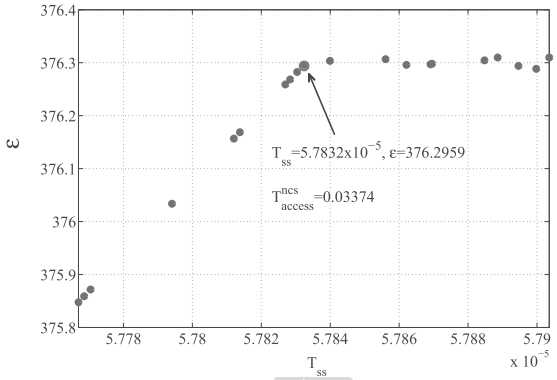

Fig. 16. Result of BFS algorithm under $M = 10$ and $N = 20$.

there are some slight differences between theoretical results and simulation results at some data points in Fig. 14. The reason is that, for CHNCS, the only impacting factor on time slots taken for successfully establishing communication links is the random time and channel of starting CH sequence, while for CHCS, another impacting factor is DCF in multi-SU contention (i.e., randomly selecting number of backoff slots). The impacts (i.e., randomly starting CH sequence and randomly selecting number of backoff slots) on number of time slots are also shown by error bar in Figs. 13 and 14.

Specifically, as shown in Fig. 13, the number of time slots consumed increases exponentially when density of pairwise SUs is increased from 10 to 150 with $M = 10$, 20 and 30. The reason is that larger number of SUs causing more collisions which leads to much more time slots to establish links. Moreover, the standard deviation (i.e., range of error bar) increases with increasing density of pairwise SUs but decreases with increasing number of channels. This is because more collisions caused by larger number of SUs leads to much patterns of establishing links. For example, pairwise SUs may take either 7000 time slots or 3000 time slots to establish a link for $M = 10$ and $N = 60$. However, when the number of channels increases, which results in reducing average number of SUs on each channel, the collisions can be relieved; thus, standard deviation decreases.

In Fig. 14, the relationship between the number of time slots and density of pairwise SUs shows basically linear with $M = 10$, 20 and 30. This can be explained by the fact that CS like DCF based CSMA/CA can further avoid collisions caused by large number of SUs on the same channel. This can be also reflected by the variation of the standard deviation which is smaller than that in Fig. 13.

Statistically, the access delay formulations of both CHNCS and CHCS can well model SU's characteristics in distributed CH-based CRNs.

B. Validation of Proposed Algorithms

The objective in this subsection is to validate the proposed algorithms. We run simulations in the scenario where $M = 10$ and $N = 20$.

Fig. 15 shows a 3-D plot of T^{ncs}_{access} varying with T_{ss} and ε, to reflect joint effects of sensing duration and detection threshold on access delay in CHNCS scenario, without considering the interference probability constraint. In Fig. 15, T_{ss} increases from $5\mu s$ to $300\mu s$ with interval of $5\mu s$, and ε increases from 5 to 1500 with interval of 5. For fixed ε, T^{ncs}_{access} first increases and then decreases and finally increases sharply with increasing T_{ss}. The difference of trends of T^{ncs}_{access} varying with ε for fixed T_{ss} is that T^{ncs}_{access} finally tends to be stable. We observe that the optimal parameters are restricted by the interference probability constraint stated in Eq. (41). Without the interference probability constraint, the optimal T_{ss} and ε both tend to 0. This indicates that, without considering PUs, SUs try to access every channel instead of operating spectrum sensing.

Fig. 16 shows the result derived from BFS algorithm under the configuration that the number of firefly is 20 and the number of iterations is 30, with the constraint that P_I is 5%. The parameters' values used in the simulation are that, β_{min} is 0.4, θ is 1 and α is 0.38. The best 'firefly' circled with red line represents that the obtained optimal T_{ss} is $57.8\mu s$, optimal ε is 376.3 and minimum T^{ncs}_{access} is $33.74ms$; the corresponding probability of detection is 90% and the corresponding probability of false detection is 13.3%.

To validate effectiveness of proposed algorithms in achieving optimal parameters and calculating minimum access delay, we compare BFS algorithm with Grid Search algorithm in terms of obtainable minimum T^{ncs}_{access}, using different computational quantities for CHNCS. We also compare SAFS with Exhaustive Search algorithm in terms of computational quantity, to obtain minimum T^{cs}_{access} for CHCS. Specifically, Grid Search is defined as that, the search is operated on T_{ss} varied from $5\mu s$ to $t_{ss}\mu s$ $(5 < t_{ss} \leq 5n, n = 1, 2, \ldots, 400)$ with interval of $(t_{ss} - 5)/N^{T_{ss}}_{itera}$ μs where $N^{T_{ss}}_{itera}$ is the number of iterations that search on T_{ss}. For each value of T_{ss}, the search on ε varies form 5 to $\varepsilon(T_{ss})$[6] with interval of $(\varepsilon(T_{ss}) - 5)/N^{\varepsilon}_{itera}$ where N^{ε}_{itera} is the number of iterations that search on ε. Thus, the computational quantity of grid search is equal to $N^{T_{ss}}_{itera} \cdot N^{\varepsilon}_{itera}$ and computational quantity of BFS is $N_F \cdot I^{Max}$ (referring to **Algorithm 1**). Exhaustive

[6] $\varepsilon(T_{ss}) = 2\mathrm{erfc}^{-1}(2 - \frac{2\bar{P}_I}{P_b})\sqrt{f_s T_{ss}(1+2\gamma)} + f_s T_{ss}(1+\gamma)$, which indicates that the search is operated under the interference probability constraint.

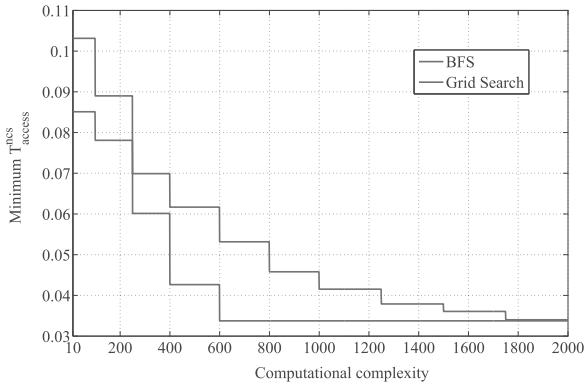

Fig. 17. BFS vs. grid search with different computational quantities.

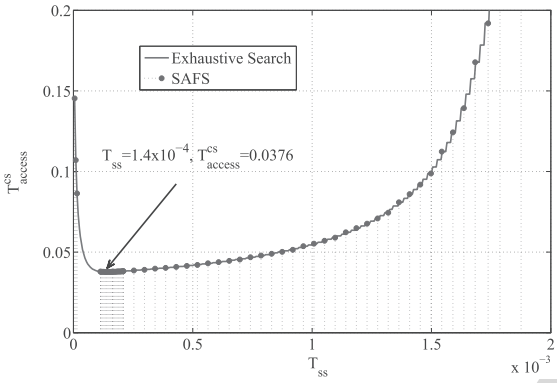

Fig. 18. Comparison between SAFS and exhaustive search in terms of minimum T^{cs}_{access}.

Search is the search operation that is executed on T_{ss} varied from $5\mu s$ to T_{slot} with interval of $5\mu s$ in CHCS scenario.

Fig. 17 shows the obtainable minimum T^{ncs}_{access} with different computational quantities when respectively using BFS and Grid Search. In Fig. 17, it shows that BFS consumes much less calculation (600 iterations of calculation) to get the optimal result than that of Grid Search (approximately 1750 iterations of calculation). The results of comparing SAFS with Exhaustive Search are shown in Fig. 18, where there are 20 SUs and 10 channels; the regular search step length and the minimum search step length in simulation are 25μs and 5μs respectively. In Fig. 18, each blue point with dotted line represents each calculation. Due to the fact that SAFS is able to neglect most redundant calculations, SAFS can save much calculation resource as well as take less time to obtain the optimal parameters and minimum access delay in the CHCS scenario. From Fig. 18, one can observe that the optimal T^{cs}_{ss} is 1.4×10^{-4}s and the corresponding T^{cs}_{access} is 0.0376s; the probability of detection and probability of false detection computed from the obtained optimal parameters are 90% and 0.5% respectively.

C. Performance Analysis

In this subsection, the objective is to analyze cost and benefit of CHNCS over CHCS with optimal parameters (i.e., T_{ss} and ε), in terms of minimum access delay and efficiency of establishing communication links.

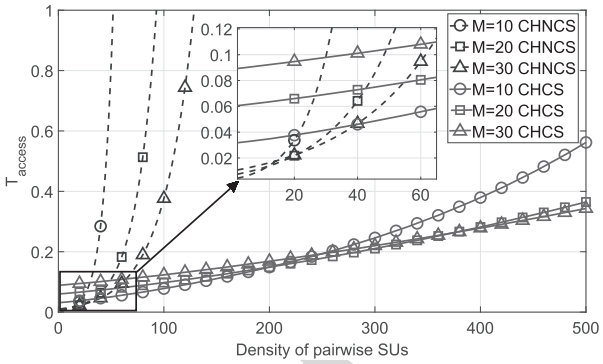

Fig. 19. Access delay performance in different scenarios.

Fig. 19 shows the minimum access delay obtained from the proposed BFS and SAFS algorithms with different density of pairwise SUs. In Fig. 19, as the density of pairwise SUs increases, access delay of both CHNCS and CHCS increases. Besides, access delay of CHNCS increases much more sharply than that of CHCS when the density of pairwise SUs increases. This can be explained by the fact that CHCS allows multiple SU senders to transmit within a time slot with CS like DCF based CSMA/CA, while CHNCS only allows one SU sender to transmit in a time slot. This indicates that, SUs in the CHCS scenario are likely to have more than one opportunity to establish links in the current time slot while SUs in the CHNCS scenario only have one opportunity. Moreover, each failed transmission causes an extra $ATSR$ time slots to achieve another rendezvous. However, it is not always effective to employ CS in CH-based distributed CRNs. In Fig. 19, it shows that access delay of CHNCS is smaller than that of CHCS when the density of pairwise SUs is small (e.g., the density of pairwise SUs is smaller than approximately 20 for $M = 10$). Furthermore, for CHNCS, access delay for $M = 10$ is larger than that for $M = 20$ when the density of pairwise SUs is larger than approximately 10. This can be explained by the fact that when density of pairwise SUs exceeds a threshold (e.g., 10 for comparing $M = 10$ and 20), multi-SU contention (i.e., P_c) impacts more on access delay than CH-based rendezvous (i.e., P_{ren} and $ATSR$). This can also explain the results of comparing $M = 10$ with 30 (threshold of density of pairwise SUs is approximately 15) and $M = 20$ with 30 (threshold of density of pairwise SUs is approximately 20). However, this 'threshold' is much larger for CHCS, e.g., for comparing $M = 10$ with 20 the threshold is approximately 200. The reason is that CS employed in the CHCS scenario can avoid contention and reduce collisions. Thus, the density of pairwise SUs needs to be large enough to reach the intensity of contention when multi-SU impacts more on access delay than CH based rendezvous.

Note that we aim to evaluate the efficiency of establishing communication links in distributed CRNs by the CH scheme. Indeed, in distributed CRNs without a central controller or a CCC, the most important step as well as the first step is to establish a link. Hence, we use communication establishing link rate (CLBR) defined as the number of communication links built by pairwise SUs per second to evaluate the

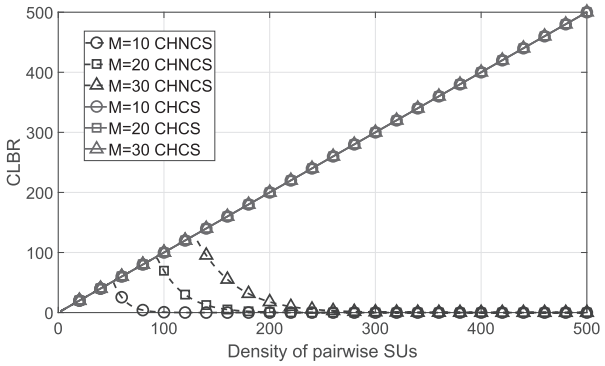

Fig. 20. CLBR performance in different scenarios.

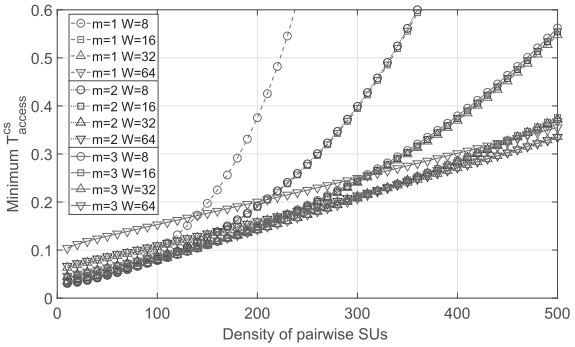

Fig. 21. Minimum access delay performance with different m and W in $M = 10$ scenario.

efficiency performance of CHNCS and CHCS. Specifically, CLBR can be calculated by

$$\text{CLBR} = \begin{cases} \dfrac{N_p}{\overline{T_{AD}}}, & \overline{T_{AD}} > 1 \\ N_p, & \text{otherwise} \end{cases}$$

where N_p is the number of pairwise SUs (i.e., density of pairwise SUs). Fig. 20 shows the performance of CLBR for both CHNCS and CHCS with increasing density of pairwise SUs. In Fig. 20, CLBR for CHNCS first increase, and then decreases as density of pairwise SUs increases from 2 to 500. However, CLBR for CHCS always increases. This can also be explained by the fact that CS allows multiple SUs to transmit in a time slot. Besides, for CHNCS, when the number of channels is larger in CRNs, the CLBR is larger with increasing density of pairwise SUs. This is because larger number of channels can ease the contention of SUs on each channel.

From Figs. 19 and 20, we can conclude that when there exist small number of SUs, it is better to not use CS in CH-based distributed CRNs.

D. Impact Analysis of MAC Parameters

The objective is to evaluate the impacts of MAC parameters (i.e., m and W) on minimum access delay for CHCS. Figs. 21 and 22 show the minimum T^{cs}_{access} varies with density of pairwise SUs in different scenarios. In the scenario that $M = 10$ in Fig. 21, the minimum T^{cs}_{access} with smaller m and W increases faster when the density of pairwise SUs increases. Although the minimum T^{cs}_{access} with smaller m and W is smaller when density of pairwise SUs is small

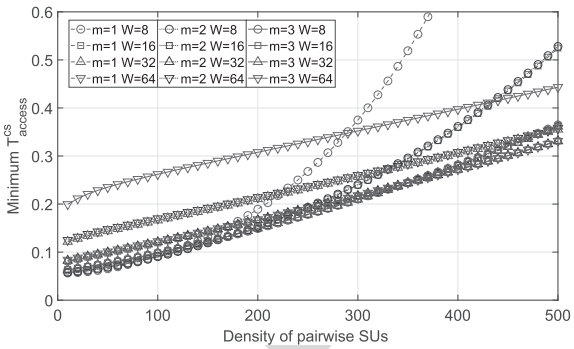

Fig. 22. Minimum access delay performance with different m and W in $M = 20$ scenario.

(e.g., approximately 140 for $m = 1$ and $W = 8$ comparing with $m = 3$ and $W = 64$), it is finally larger than that with larger m and W with increasing density of pairwise SUs. However, in the scenario that $M = 20$ in Fig. 22, the minimum T^{cs}_{access} with larger m and W is much larger than that with smaller m and W when density of pairwise SUs is small (e.g., approximately 280 for $m = 1$ and $W = 8$ comparing with $m = 3$ and $W = 64$). This can be explained as follows. When the number of SUs on each channel is small, the CH-based rendezvous impacts more than multi-SU contention, but CH-based rendezvous impacts less than multi-SU contention when the number of SUs on each channel is large.

VIII. Conclusion

This paper proposes a tradeoff problem between spectrum sensing duration and time slot duration for CHNCS and a tradeoff problem between spectrum sensing duration and contention transmission duration for CHCS, in distributed CRNs from a cross-layer perspective. For both scenarios, imperfect spectrum sensing in PHY layer and CH-based rendezvous in MAC layer are jointly taken into consideration. Specifically, we first derive the exact expressions of the probability that SUs access channels being aware of the impact of imperfect spectrum sensing. Then, by jointly considering the impact of imperfect spectrum sensing and CH-based rendezvous algorithm, we employ an absorbing Markov chain to model the multi-SU contention transmission process for CHCS and derive the probability of SUs successfully exchanging rendezvous information for both scenarios. Furthermore, we formulate the corresponding access delay models for both CHNCS and CHCS with the constraint of interference probability to protect PUs' activities. Finally, we propose a bio-inspired algorithm to search for the optimal parameters (i.e., sensing duration and detection threshold) for CHNCS and propose a self-adaptive step length algorithm to search for the optimal sensing duration for CHCS. Numerical simulation results show that (i) the theoretical results obtained from access delay models for CHNCS and CHCS both match simulation results well, which indicates that the access delay models for both scenarios well simulate SUs establishing communication link in distributed CRNs; (ii) both BFS algorithm and SAFS algorithm can effectively obtain the optimal parameters of minimum access delay with consuming less computational resource; (iii) in terms of access delay,

when there exist fewer SUs (e.g., 20 for $M = 10$) the access delay of CHNCS is smaller than that of CHCS. However, when the number of SUs increases, the access delay of CHNCS increases more rapidly than that of CHCS. Besides, it can be concluded that with the number of SUs increasing multi-SU contention impacts more than CH based rendezvous on access delay; (iv) in term of CLBR, due to the intense collisions caused by increasing SUs, CLBR of CHNCS has worse performance than that of CHNCS; (v) similarly in conventional IEEE 802.11 DCF based wireless networks, proper values of m and W can effectively avoid the contention and collision caused by large number of SUs.

REFERENCES

[1] N. C. Theis, R. W. Thomas, and L. A. DaSilva, "Rendezvous for cognitive radios," *IEEE Trans. Mobile Comput.*, vol. 10, no. 2, pp. 216–227, Feb. 2011.

[2] P. M. R. dos Santos, M. A. Kalil, O. Artemenko, A. Lavrenko, and A. Mitschele-Thiel, "Self-organized common control channel design for cognitive radio ad hoc networks," in *Proc. IEEE PIMRC*, Sep. 2013, pp. 2419–2423.

[3] K. G. M. Thilina, E. Hossain, and D. I. Kim, "DCCC-MAC: A dynamic common-control-channel-based MAC protocol for cellular cognitive radio networks," *IEEE Trans. Veh. Technol.*, vol. 65, no. 5, pp. 3597–3613, May 2016.

[4] A. M. Masri, C. F. Chiasserini, C. Casetti, and A. Perotti, "Common control channel allocation in cognitive radio networks through UWB communication," *J. Commun. Netw.*, vol. 14, no. 6, pp. 710–718, Dec. 2012.

[5] X. J. Tan, C. Zhou, and J. Chen, "Symmetric channel hopping for blind rendezvous in cognitive radio networks based on union of disjoint difference sets," *IEEE Trans. Veh. Technol.*, vol. 66, no. 11, pp. 10233–10248, Nov. 2017.

[6] R. Paul and Y.-J. Choi, "Adaptive rendezvous for heterogeneous channel environments in cognitive radio networks," *IEEE Trans. Wireless Commun.*, vol. 15, no. 11, pp. 7753–7765, Nov. 2016.

[7] K. Bian and J.-M. Park, "Maximizing rendezvous diversity in rendezvous protocols for decentralized cognitive radio networks," *IEEE Trans. Mobile Comput.*, vol. 12, no. 7, pp. 1294–1307, Jul. 2013.

[8] H. Liu, Z. Lin, X. Chu, and Y.-W. Leung, "Jump-stay rendezvous algorithm for cognitive radio networks," *IEEE Trans. Parallel Distrib. Syst.*, vol. 23, no. 10, pp. 1867–1881, Oct. 2012.

[9] J. Li, H. Zhao, J. Wei, D. Ma, and L. Zhou, "Sender-jump receiver-wait: A simple blind rendezvous algorithm for distributed cognitive radio networks," *IEEE Trans. Mobile Comput.*, vol. 17, no. 1, pp. 183–196, Jan. 2018.

[10] C.-M. Chao, H.-Y. Fu, and L.-R. Zhang, "A fast rendezvous-guarantee channel hopping protocol for cognitive radio networks," *IEEE Trans. Veh. Technol.*, vol. 64, no. 12, pp. 5804–5816, Dec. 2015.

[11] *Standard for Information Technology—Local and Metropolitan Area Networks - Specific Requirements—Part 22: Cognitive Radio Wireless Regional Area Networks (WRAN) Medium Access Control (MAC) and Physical Layer (PHY) Specifications: Policies and Procedures for Operation in the Bands that Allow Spectrum Sharing where the Communications Devices May Opportunistically Operate in the Spectrum of the Primary Service*, IEEE Standard 802.22, 2011. [Online]. Available: http://grouper.ieee.org/groups/802/22

[12] S. Zhang, A. S. Hafid, H. Zhao, and S. Wang, "Cross-layer rethink on sensing-throughput tradeoff for multi-channel cognitive radio networks," *IEEE Trans. Wireless Commun.*, vol. 15, no. 10, pp. 6883–6897, Oct. 2016.

[13] X.-S. Yang, "Firefly algorithms for multimodal optimization," in *Stochastic Algorithms: Foundations and Applications*. Berlin, Germany: Springer, 2009, pp. 169–178.

[14] S. Wang, J. Zhang, and L. Tong, "A characterization of delay performance of cognitive medium access," *IEEE Trans. Wireless Commun.*, vol. 11, no. 2, pp. 800–809, Feb. 2012.

[15] Z. Liang, S. Feng, D. Zhao, and X. S. Shen, "Delay performance analysis for supporting real-time traffic in a cognitive radio sensor network," *IEEE Trans. Wireless Commun.*, vol. 10, no. 1, pp. 325–335, Jan. 2009.

[16] W. Li, X. Cheng, T. Jing, Y. Cui, K. Xing, and W. Wang, "Spectrum assignment and sharing for delay minimization in multi-hop multi-flow CRNs," *IEEE J. Sel. Areas Commun.*, vol. 31, no. 11, pp. 2483–2493, Nov. 2013.

[17] Q. Liu, X. Wang, B. Han, X. Wang, and X. Zhou, "Access delay of cognitive radio networks based on asynchronous channel-hopping rendezvous and CSMA/CA MAC," *IEEE Trans. Veh. Technol.*, vol. 64, no. 3, pp. 1105–1119, Mar. 2015.

[18] S. E. Safavi and K. P. Subbalakshmi, "Effective bandwidth for delay tolerant secondary user traffic in multi-PU, multi-SU dynamic spectrum access networks," *IEEE Trans. Cogn. Commun. Netw.*, vol. 1, no. 2, pp. 175–184, Jun. 2015.

[19] D. Zhang, T. He, F. Ye, R. K. Ganti, and H. Lei, "Neighbor discovery and rendezvous maintenance with extended quorum systems for mobile applications," *IEEE Trans. Mobile Comput.*, vol. 16, no. 7, pp. 1967–1980, Jul. 2017.

[20] C. de Sousa, D. Passos, R. C. Carrano, and C. V. Albuquerque, "Multichannel continuous rendezvous in cognitive networks," in *Proc. ACM MSWiM*, 2017, pp. 63–70.

[21] X. Liu and J. Xie, "A practical self-adaptive rendezvous protocol in cognitive radio ad hoc networks," in *Proc. IEEE INFOCOM*, Apr./May 2014, pp. 2085–2093.

[22] Y.-C. Liang, Y. Zeng, E. C. Y. Peh, and A. T. Hoang, "Sensing-throughput tradeoff for cognitive radio networks," *IEEE Trans. Wireless Commun.*, vol. 7, no. 4, pp. 1326–1337, Apr. 2008.

[23] M. A. Hossain and N. I. Sarkar, "A distributed multichannel MAC protocol for rendezvous establishment in cognitive radio ad hoc networks," *Ad Hoc Netw.*, vol. 70, pp. 44–60, Mar. 2018.

[24] K. Tan, H. Liu, J. Zhang, Y. Zhang, J. Fang, and G. M. Voelker, "Sora: High-performance software radio using generalpurpose multi-core processors," *Commun. ACM*, vol. 54, no. 1, pp. 99–107, Jan. 2011.

[25] C. Cordeiro, K. Challapali, and D. Birru, "IEEE 802.22: An introduction to the first wireless standard based on cognitive radios," *J. Commun.*, vol. 1, no. 1, pp. 38–47, Apr. 2006.

[26] H. Zhao, K. Ding, N. I. Sarkar, J. Wei, and J. Xiong, "A simple distributed channel allocation algorithm for D2D communication pairs," *IEEE Trans. Veh. Technol.*, vol. 67, no. 11, pp. 10960–10969, Nov. 2018.

[27] X. Liu and J. Xie, "A slot-asynchronous MAC protocol design for blind rendezvous in cognitive radio networks," in *Proc. IEEE Globecom*, Dec. 2014, pp. 4641–4646.

[28] K. H. Rosen, "Counting," in *Discrete Mathematics and Its Applications*, 7th ed. New York, NY, USA: McGraw-Hill, 2012, pp. 407–434.

[29] G. Bianchi, "Performance analysis of the IEEE 802.11 distributed coordination function," *IEEE J. Sel. Areas Commun.*, vol. 18, no. 3, pp. 535–547, Mar. 2000.

[30] D. P. Bertsekas and J. N. Tsitsiklis, "Markov Chains," in *Introduction to Probability*, 2th ed. Nashua, NH, USA: Athena Scientific, 2008, pp. 339–405.

Jiaxun Li received the B.S. and M.S. degrees from the National University of Defense Technology (NUDT), Changsha, China, in 2013 and 2015, respectively, where he is currently pursuing the Ph.D. degree, all in information and communication engineering. He visited the Ph.D. Student at the University of Montreal, Canada, from 2017 to 2018. He has served as a Reviewer for many international journals such as the IEEE SYSTEM JOURNAL, the IEEE COMMUNICATION LETTER, and the *IEEE Communication Magazine*. His main research interests include cognitive radio networks and resource optimization.

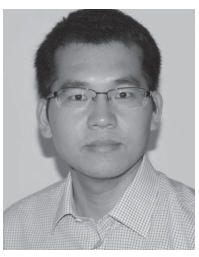

Haitao Zhao (M'13–SM'18) received the M.S. and Ph.D. degrees in information and communication engineering from the National University of Defense Technology (NUDT), Changsha, China, in 2004 and 2009, respectively. He has visited the Institute of Electronics, Communications and Information Technology, Queens University Belfast, U.K., from 2008 to 2009, and conducted post-doctoral research with Hong Kong Baptist University from 2014 to 2015. He is currently a Professor with the College of Electronic Science and Engineering, NUDT. His main research interests include cognitive radio networks, self-organized networks, and cooperative communications. He is currently a member of the ACM, Worldwide University Network Cognitive Communications Consortium, and also a Mentor Member of the IEEE 1900.1 standard. He has served as a TPC Member of the IEEE ICC from 2014 to 2019 and GLOBECOM 2015 to 2019. He has served as a guest editor for several international journal special issues on cognitive radio networks.

Shaojie Zhang received the M.S. and Ph.D. degrees in information and communication engineering from the National University of Defense Technology, Changsha, China, in 2012 and 2016, respectively. He is currently a Lecturer with the Army Aviation Institute of PLA, Beijing, China. His current research interests include cognitive radio networks and performance analysis and optimization.

Abdelhakim Senhaji Hafid was a Senior Research Scientist with Bell Communications Research (Bellcore), NJ, USA, where he spent several years focusing on the context of major research projects on the management of next generation networks. He is currently a Full Professor with the University of Montreal. He is also the Founding Director of the Network Research Laboratory and the Montreal Blockchain Laboratory. He is a Research Fellow of CIRRELT, Montreal, Canada. He has extensive academic and industrial research experience in the areas of management and design of next generation networks. His current research interests include IoT, fog/edge computing, blockchain, and intelligent transport systems.

Dusit Niyato (M'09–SM'15–F'17) received the B.Eng. degree from the King Mongkuts Institute of Technology Ladkrabang, Thailand, in 1999, and the Ph.D. degree in electrical and computer engineering from the University of Manitoba, Canada, in 2008. He is currently a Professor with the School of Computer Science and Engineering, Nanyang Technological University, Singapore. His research interests are in the areas of energy harvesting for wireless communication, the Internet of Things, and sensor networks.

Jibo Wei received the B.S. and M.S. degrees from the National University of Defense Technology (NUDT), Changsha, China, in 1989 and 1992, respectively, and the Ph.D. degree from Southeast University, Nanjing, China, in 1998, all in electronic engineering. He is currently a Professor with the Department of Communication Engineering, NUDT. His research interests include wireless network protocol and signal processing in communications, cooperative communication, and cognitive network. He is a Member of the IEEE Communication Society and the IEEE VTS. He is a Senior Member of the China Institute of Communications and Electronics. He is also an Editor of the *Journal of China Communications*.